DANMARKS OG GRØNLANDS GEOLOGISKE UNDERSØGELSE RAPPORT 2010/120

The Tartoq Group, SW Greenland: Mineralogy, textures and a preliminary metamorphic to hydrothermal history

Vincent J. van Hinsberg, Kristoffer Szilas & Alex F. M. Kisters

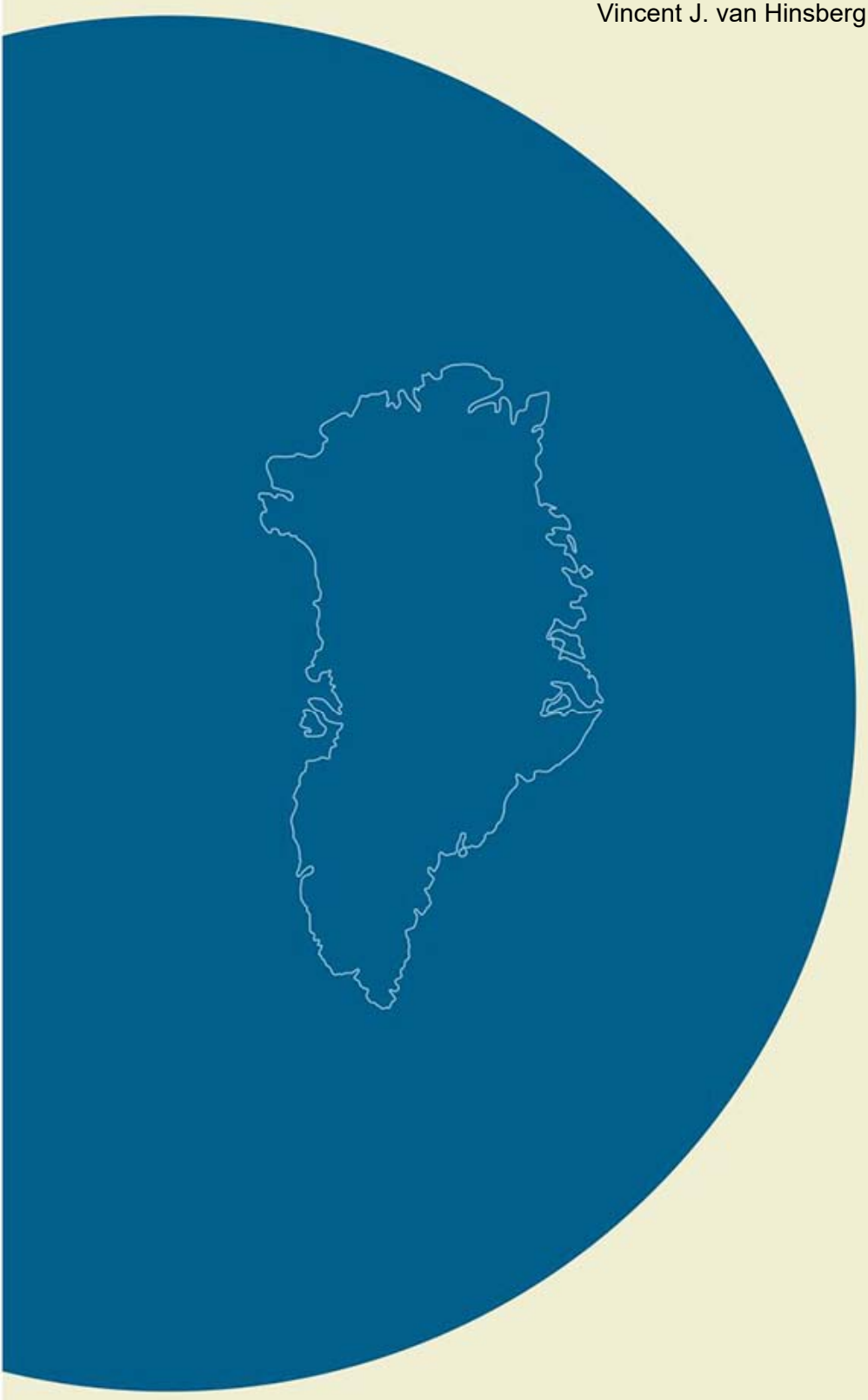

GEOLOGICAL SURVEY OF DENMARK AND GREENLAND
MINISTRY OF CLIMATE AND ENERGY

GEUS

DANMARKS OG GRØNLANDS GEOLOGISKE UNDERSØGELSE RAPPORT 2010/120

The Tartoq Group, SW Greenland: Mineralogy, textures and a preliminary metamorphic to hydrothermal history

Vincent J. van Hinsberg[1], Kristoffer Szilas[2] & Alex F. M. Kisters[3]

[1] Department of Earth Sciences, University of Oxford, South Park Road, Oxford, United Kingdom
[2] Geological Survey of Denmark and Greenland (GEUS), Øster Voldgade 10, 1350 København, Denmark
[3] Department of Earth Sciences, Stellenbosch University, Cnr Ryneveld and Merriman Streets, Stellenbosch, Western Cape, South Africa

GEOLOGICAL SURVEY OF DENMARK AND GREENLAND
MINISTRY OF CLIMATE AND ENERGY

GEUS

Introduction

The Tartoq Group covers a series of supracrustal blocks along the Sermiligaarsuk Fjord in South-West Greenland (Fig. 1). The Tartoq Group supracrustal rocks are low to high-grade, mostly mafic, greenschists and amphibolites of Archaean age (>2944 Ma - Nutman & Kalsbeek 1994), bounded by unconformable contacts with their enclosing TTG gneisses. They have locally been intruded by TTG and pegmatite melts (Nutman & Kalsbeek 1994, and our own work) and are cut by dykes of intermediate to ultramafic composition with ages ranging from early Proterozoic, to Gardar stage Middle Proterozoic, to Mesozoic (Higgins 1990). In the east, the Tartoq supracrustals are overlain by younger Ketilidian rocks separated by a westward thrusted unconformity (Higgins 1990; Garde *et al.* 1998).

The Tartoq Group supracrustal rocks have been universally affected by hydrothermal activity, which encompasses a number of different stages and culminates in the formation of gold-bearing sulfide mineralizations. The associated economic potential has led to extensive work on the Tartoq Group from the 1970s onward, including detailed geological mapping, soil, sediment and rock geochemistry, and geophysical surveys (Geisler 1972; Geisler 1975; King 1983, 1985; Appel & Secher 1984; Petersen 1991, 1992; Evans & King 1993; Petersen & Madsen 1995; Steenfelt 2000).

In this contribution we describe the mineralogy and textures of the Tartoq Group supracrustals, constrain the conditions of their formation, and present a preliminary metamorphic to hydrothermal history for these rocks.

Geology of the Tartoq Group

Lithologies and textures

The Tartoq Group includes a wide variety of lithologies, which is related both to a diverse suite of precursors, and to a large range of conditions to which these units were subsequently subjected. Lithologies are shared between blocks and the overall Tartoq Group displays a homogenous suite of lithologies. The most common lithologies are greenstones/greenschists, amphibolites and felsic schists/gneisses. Aside from these major lithologies, the Tartoq Group supracrustals also includes meta-sediments, ultramafic rocks and minor calc-silicates (Fig. 2). Detailed descriptions of the lithologies in Nuuluk and Iterlak, especially those related to the hydrothermal stages of the Tartoq's development are further found in King (1985), and Petersen (1991, 1992).

Greenstones and greenschists

Tartoq Group greenschists and greenstones encompass fine- to coarse-grained rocks of low to medium metamorphic grade with a dominant mineralogy of chlorite, plagioclase, quartz, ilmenite, carbonate ± epidote ± actinolite. As grade increases, calcic amphibole appears and becomes progressively more important. Locally, magnetite is a major constituent (e.g. north-central Nuuluk, stations 10ViVH045-048). Accessory phases include tourmaline and apatite. Relict minerals are common and include clino-pyroxene, spinel and plagioclase. The main difference between the greenschists and greenstones is the presence of a metamorphic fabric, with a pervasive schisteous chlorite foliation in the greenschists accompanied by a

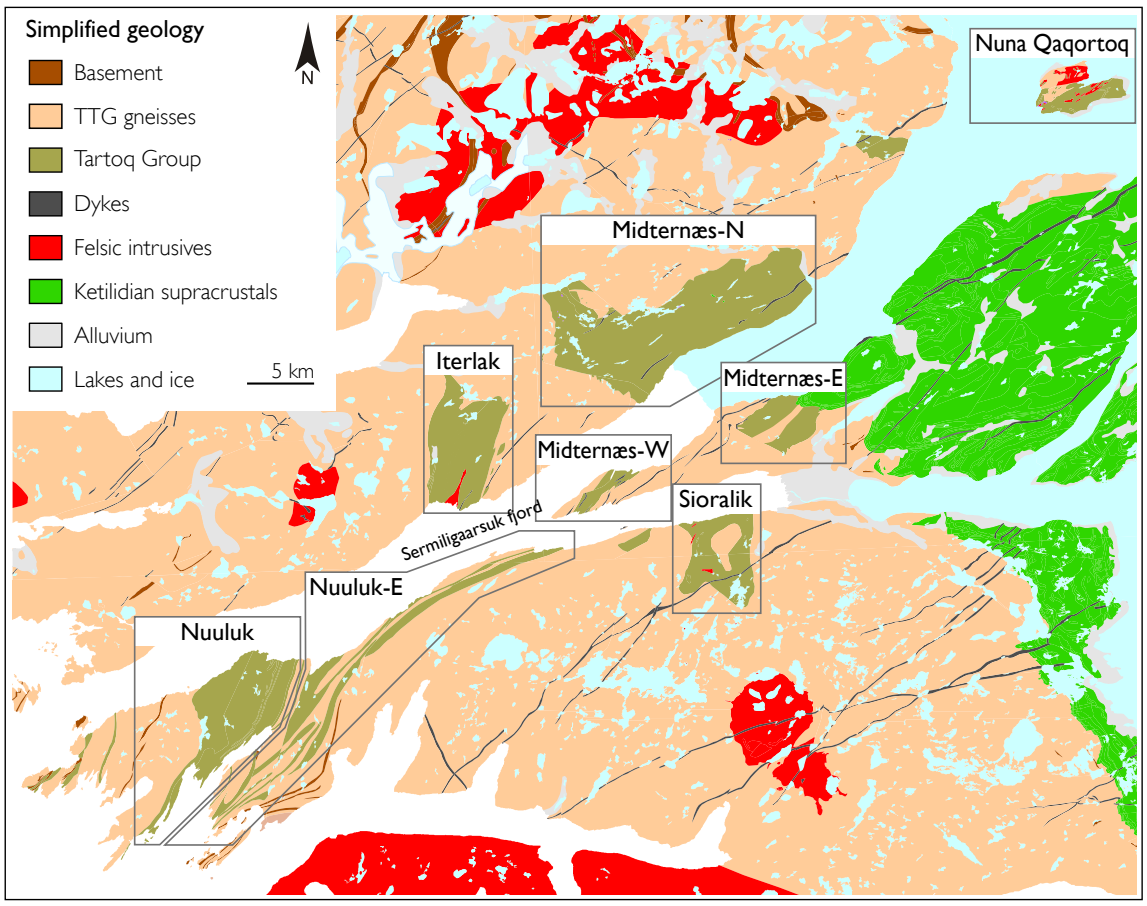

Figure 1. Overview map of the Tartoq Group in SW Greenland outlining the Tartoq blocks that are discussed in this report. Names for the different Tartoq blocks are after King (1985). Map modified after GEUS geological maps (Henriksen 1968, Escher & Jensen 1974, Jensen 1975).

complete overprint of original textures, whereas the greenstones are massive with little or weak development of a foliation and common preservation of original (magmatic) textures. Gradual transitions from greenstone to greenschist are commonly observed in Nuuluk and may indicate that most of the greenschists represent metamorphosed and deformed greenstones. However, there is substantial mineralogical and textural heterogeneity within both the greenstones and greenschists, and deformation is likely to have taken advantage of this.

The greenschists display a characteristic texture throughout the Tartoq Group that will be referred to here as a "knobbly texture" (Figs. 3a-d). This texture is characterized by irregular knobbly surfaces on outcrops (sub)parallel to the foliation, with abundant voids in between wedge-shaped fragments. This wedge-shape results from a penetrative network of carbonate veinlets enclosing fragments of greenschist, and subsequent preferential carbonate weathering. The formation of this carbonate network is related to deformation, with one direction of carbonate veining sub-parallel to the foliation direction, and the second, intersection direction filling extensional gashes (Petersen 1992). The prominence of this texture is directly linked to the deformation intensity and carbonate content (cf. Fig 3a-c).

Where the greenschists and greenstones are caught up in thrusting, they develop a laminated, fine-grained appearance (Fig. 3e). These laminated rocks lack the schistose foliation, and carbonate is absent. They are further silicified, which can give them a chert-like appearance.

Amphibolites

The Tartoq Group amphibolites range from fine-grained low-grade amphibolites on Nuna Qaqortoq to coarse-grained high-grade mafic to felsic amphibolites in Sioralik. Calcic amphibole, plagioclase and quartz are the dominant constituent minerals, with magnetite or ilmenite as the main accessory phases. At lower grades, epidote and chlorite are common, whereas at higher grades diopside and eventually garnet were identified. At one locality in Sioralik, conditions reach the wet solidus and partial melts develop, as well as leucocratic rims on garnet (Figs. 3f,g). Anatexis was also reported for these rocks by Evans & King (1993).

The amphibolites vary in composition from mafic to felsic, and are dominated by amphibole or plagioclase respectively. Leucocratic layers in mafic amphibolite, and vice versa, have also been identified (e.g. Fig. 3h). Amphiboles are light to dark green in colour, and where black amphibole is observed it appears to represent later overprint related to hydrothermal veining.

The textures of the amphibolite vary along with their grade from schistose at low grade where the foliation is made up of chlorite, to a gneissic banding at high grade with separation of the amphibole and quartz + plagioclase components. Primary gabbroic textures are also common, and most amphibolite gneisses grade to a gabbroic texture in less deformed parts. Retrograde replacement of amphiboles by chlorite has been observed in a number of settings, including intrusion of pegmatites (e.g. Sioralik), surrounding hydrothermal veins (e.g. Iterlak) and adjacent to cross-cutting dykes (e.g. Midternæs-E).

Felsic schists and gneisses

Sheets of felsic gneisses are present throughout the Tartoq Group and are most pronounced in Nuuluk (the felsic sheet in the cliff west of the central valley - Fig. 3i), Iterlak (multiple sheets of variable width on the central plateau) and Midternæs-E (a wide felsic unit separating the plateau in the south from the broad northern valley). These felsic sheets have a mineralogy of plagioclase + quartz + ilmenite ± K-feldspar ± muscovite. Biotite is rare. They are characterized by intense deformation, with development of a mylonitic texture, although thick sheets grade into a less deformed core. Where muscovite is common, these rocks have a schistose appearance, but more commonly they display gneissic banding.

Ultramafic rocks

Ultramafic rocks are widespread in the Tartoq Group. They occur both as isolated lenses (e.g. in Midternæs-N and on Nuna Qaqortoq), and as semi-continuous layers with lenses along these (e.g. eastern Iterlak and southern Midternæs-E). The ultramafic rocks are remarkably similar in their textures and mineralogy, as well as in the mineralogy of the reaction rim to their host rocks. In their most complete extent, they comprise a core of massive antigorite serpentine + magnetite (+ olivine in Sioralik), enveloped in concentric layers of green actinolite ± chlorite ± serpentine and light gray talc + carbonate + magnetite schists (Fig. 3j,k). The green intermediate layer can be absent or split into pure actinolite, and chlorite + serpentine layers. Serpentine pseudomorphs after pyroxene were observed in the core of

► Figure 2 (as appendix map). Detailed geological maps of the different Tartoq blocks based on original Geus maps (Henriksen 1968, Escher & Jensen 1974, Jensen 1975) updated with mapping reported in Geisler (1975), King (1983, 1985), Petersen (1991, 1992), Evans and King (1993) and our own work.

the Midternæs-N body, and these give the rock a crystal-supported cumulate texture. During deformation, the magnetite in the ultramafic lenses is commonly segregated into bands (Fig 3l), as was also noted by King (1985).

Talc schist is the most abundant component and in many cases is the only remnant of the original ultramafic body. It has a strong foliation that is invariably late and, where late folding has occurred, is parallel to the axial plane of these folds. Light gray talc encloses idiomorphic crystals of pale yellow carbonate up to cm-sized, which weather to a distinct orange colour (Fig. 3k). The talc schists are locally strongly magnetic and contain magnetite crystals up to 5 mm in size and idiomorphic in shape.

Deviations from this general texture and mineralogy were observed for the ultramafic lens on Nuna Qaqortoq, where anthophyllite is found in reaction rims with cross-cutting pegmatites, and for one lens in Sioralik (station 10ViVH168), where magnetite outlines serpentine pseudomorphs after ortho-amphibole that developed on the surface of the ultramafic lens during metamorphism (Fig. 3m). Although this texture somewhat resembles spinifex texture, the segregation of the magnetite indicates that it is rather a secondary texture, because magnetite only develops upon serpentinisation of primary olivine and was therefore not available for segregation prior to this conversion.

Meta-sediments

Conclusive evidence for sediments is limited in the Tartoq Group at present (see below). Earlier work interpreted the knobbly texture of the greenschists as representing pyroclastics, and the felsic units as volcanic tuffs or TTG derived sediments (e.g. Higgins 1968, 1990; Geisler 1972; Berthelsen & Henriksen 1975; King 1983, 1985; Apple & Secher 1984; Petersen 1991, 1992). However, our observations show that these interpretations should be treated with caution, and that at least at several locations are incorrect, in agreement with suggestions by King (1985) and Petersen (1992). The felsic unit of central Nuuluk, for example, is re-interpreted here as a sliver of TTG basement that was sheared into the Tartoq Group supracrustals (see below), and the intense hydrothermal overprint on the greenschists makes it difficult to conclusively establish their protolith.

► Figure 3. Photographs of characteristic textures of Tartoq Group supracrustal rocks: a-d greenschists with progressive development of a characteristic knobbly weathering texture with increasing content an intersecting network of carbonate veins; e laminated silicified greenschist in a thrust zone in central Nuuluk giving the rock a chert-like appearance; f-g high-grade amphibolites in Sioralik with plagioclase rimmed garnet and development of partial melts that here break through a fold hinge; h felsic layer in banded amphibolite in Sioralik; i mylonitic gneiss sheet in cliff face of central Nuuluk; j-k talc schist alteration of serpentinised ultramafic lenses in Iterlak with large carbonate grains. A metasomatic rim on contact with gabbroic amphibolites is invariably present and is dominated by actinolite; l segregation of magnetite into bands in a serpentinised ultramafic lens in Midternæs-N; m pseudomorphs of antigorite after amphibole outlined by magnetite on the surface of an ultramafic lens in Sioralik; n sample of sedimentary Banded Iron Formation in northern Iterlak; o strongly altered foot wall of thrust zone in Nuuluk showing channelling of fluids into thrust zones; p late-stage quartz-ankerite vein with restitic bright green fuchsite on vein walls; q cataclasite zone with feldspar clasts floating in a matrix of chlorite; r-s lenticular structures in amphibolites of Iterlak and Nuna Qaqortoq respectively that resemble pillows; t-u sills in knobbly greenschist in Nuuluk with commonly sharp contacts suggesting a protolith contrast rather than progressive carbonation; v sill of intermediate composition fingering into greenschist; w folded low-grade rocks in Nuuluk-E with original bedding recognised by colour contrasts. An original foliation that is parallel to this bedding is overprinted by a foliation that is axial planar to these folds.


a
b
c
d
e
f
g
h


i
j
k
l
m
n
o

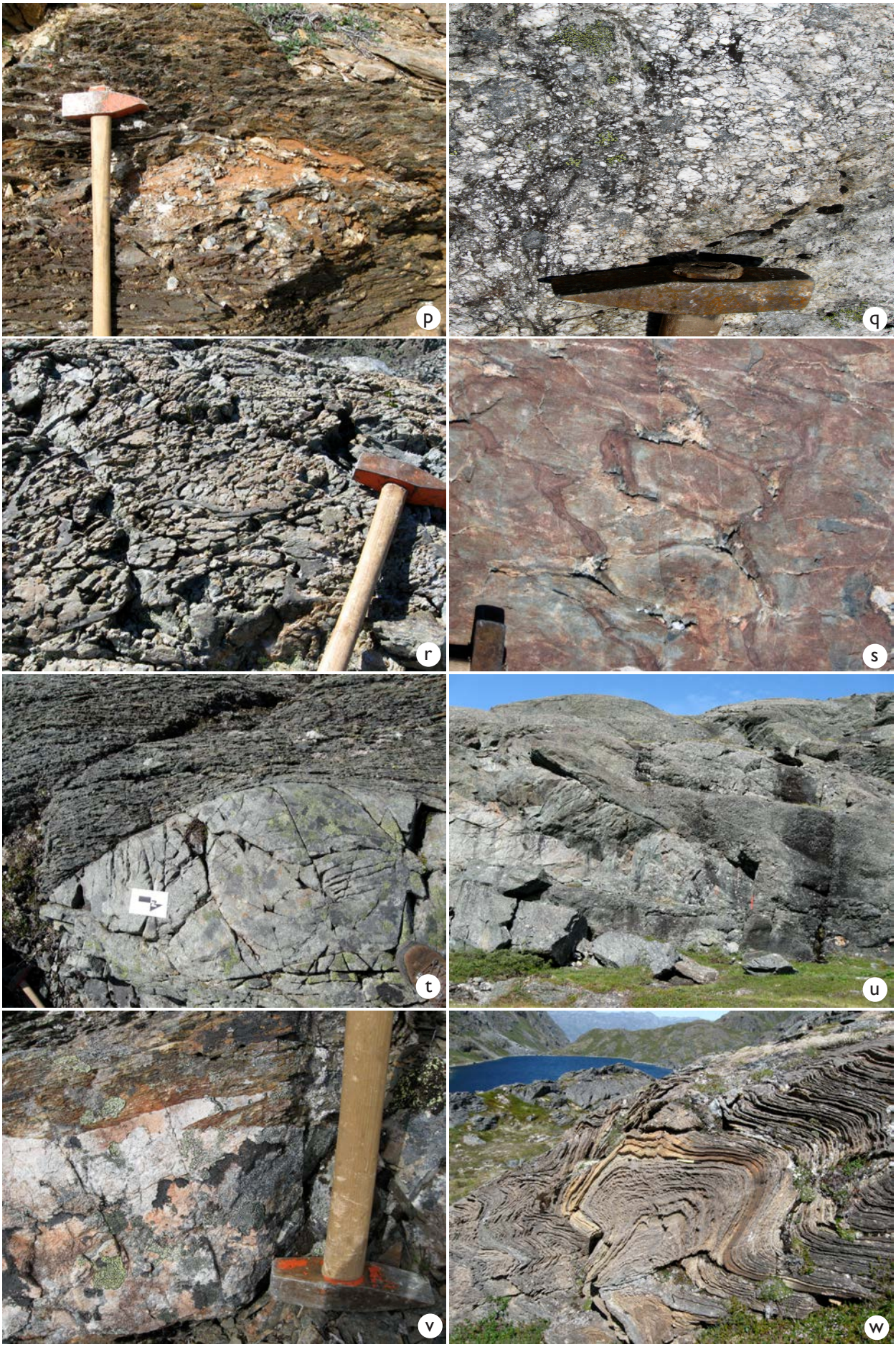
p
q
r
s
t
u
v
w

Direct evidence for sediments is present in the form of a small Banded Iron Formation in North Iterlak (Fig. 2b - a detailed map of this location is presented by King 1985). The BIF is strongly folded with steeply plunging folds and occurs in a sequence with fine-grained knobbly greenschist on its southern contact and a light-coloured felsic schist on its northern contact. A thin layer of greenschist is also interbedded with the BIF. The BIF itself is approximately 10 m thick and consists of regular mm thick layers of alternating magnetite and quartz (Fig. 3n). Several pink carbonate layers are present within the BIF package and their regular nature and consistent thickness suggests these to be primary.

Calc-silicates

Minor calc-silicates have been observed throughout the Tartoq Group, where they are most readily identified by the presence of abundant diopside. They generally occur as discontinuous, light green coloured layers and lenses in amphibolite, with the most extensive outcrop being a 10 m thick garnet + diopside + plagioclase + amphibole layer in Sioralik (Figs. 2 and 3j). At lower grade, epidote, rather than garnet is present. These calc-silicate rocks do not represent metamorphism of carbonated greenschists or amphibolites, because this event post-dates metamorphism as will be discussed below.

Hydrothermal overprint

The original lithologies are universally affected by later hydrothermal activity, albeit to variable degrees of intensity. This hydrothermal overprint can be separated into several stages, and it is unlikely that these represent a continuous episode of activity. The first stage of activity is the most pervasive and widespread, and is characterized by carbonation. Its imprint is most pronounced for the greenschists/greenstones and ultramafic rocks, with the appearance of a pervasive network of carbonates in the greenschists and development of their knobbly texture, and the formation of the talc-carbonate reaction rims on the ultramafic bodies. Carbonate veins and carbonate-rich layers are, however, also observed in amphibolites and in the felsic gneisses and schists. Depending on bulk rock composition, the carbonate mineralogy varies from calcite, to dolomite, to ankerite. Carbonate is commonly accompanied by small (mm-sized) idiomorphic grains of tourmaline, which occur as isolated dispersed grains. Tourmaline colour is highly variable from brown to green to blue, depending on the composition of its host rock, and sector zoning is common.

The spatial distribution of carbonate schists, greenschists and greenstones in eastern Nuuluk is that of an anastomosing network enclosing lenses of greenstone (Fig. 4).We interpret this anastomosing network as a direct representation of the pathways of the hydrothermal carbonate-bearing fluid, with progressive channelling of the these fluids resulting in the transition from greenschist to carbonate schist and development of greenstone "islands".

Later hydrothermal activity is more focussed and centres on thrust planes and their associated foot wall. The overprint is generally intense and may completely overprint the original lithology. Foot wall rocks are commonly light in colour and display silicification and carbonation (Fig 3o). In K-bearing lithologies, and at the base of the felsic sheet in central Nuuluk (Fig. 2), extensive muscovite is introduced during alteration, producing a friable muscovite-chlorite schist with abundant carbonate. Chalcopyrite, or pyrite + pyrrhotite are also common, and graphite associated with these zones has been observed in northern Nuuluk (station 10ViVH044, see also Petersen 1992). Introduction of sulfides culminates in the de-

velopment of massive pyrite and arsenopyrite layers after Fe-rich lithologies. These include the magnetite-rich greenschist in central Nuuluk (Fig. 2) and the banded magnetite rocks of Iterlak (see also Appel & Secher 1984). It is this final stage that is associated with the most elevated gold showings (Appel & Secher 1984; King 1985; Petersen 1991, 1992; Evans & King 1993).

The centre of the carbonate schist commonly contains irregular quartz-ankerite veins with fuchsite developing on vein walls (Fig. 3p). These veins are most pronounced in the Western and Eastern Carbonate Zones, and Felsic Tuff Zone of Nuuluk (see King 1983, 1985; Petersen 1992; and Fig. 2). The veins locally crosscut the carbonate schist foliation and are therefore late, and we interpret them as co-genetic with foot wall alteration in thrust zones.

Structure

Two structural domains are present in the Tartoq Group; a thrusting dominated domain, and a series of strike-slip domains. The differences are readily identifiable from the topography of the different blocks, with strike-slip dominated blocks characterized by steep narrow valleys and ridges parallel to the near-vertical foliation, e.g. Midternæs and the Tartoq Group slivers south of Sermiligaarsuk Fjord. Thrusting dominates in Nuuluk and Iterlak and is associated with folding, especially in Iterlak. Dips are more shallow, leading to open valleys bordering plateaus. Nuuluk and Sioralik both represent a klippe on top of TTG gneisses, whereas Iterlak was overthrust by TTG gneiss on its western contact (Fig. 5).

Internal thrust planes in the greenschists are observed and are associated with development of a laminated and silicified rock (Fig. 3e), as well as extensive hydrothermal overprinting (e.g. Fig. 4). However, overall, thrusting is concentrated on felsic units, including the cliff of felsic material in central Nuuluk and the parallel bands of felsic material in Iterlak. The deforma-

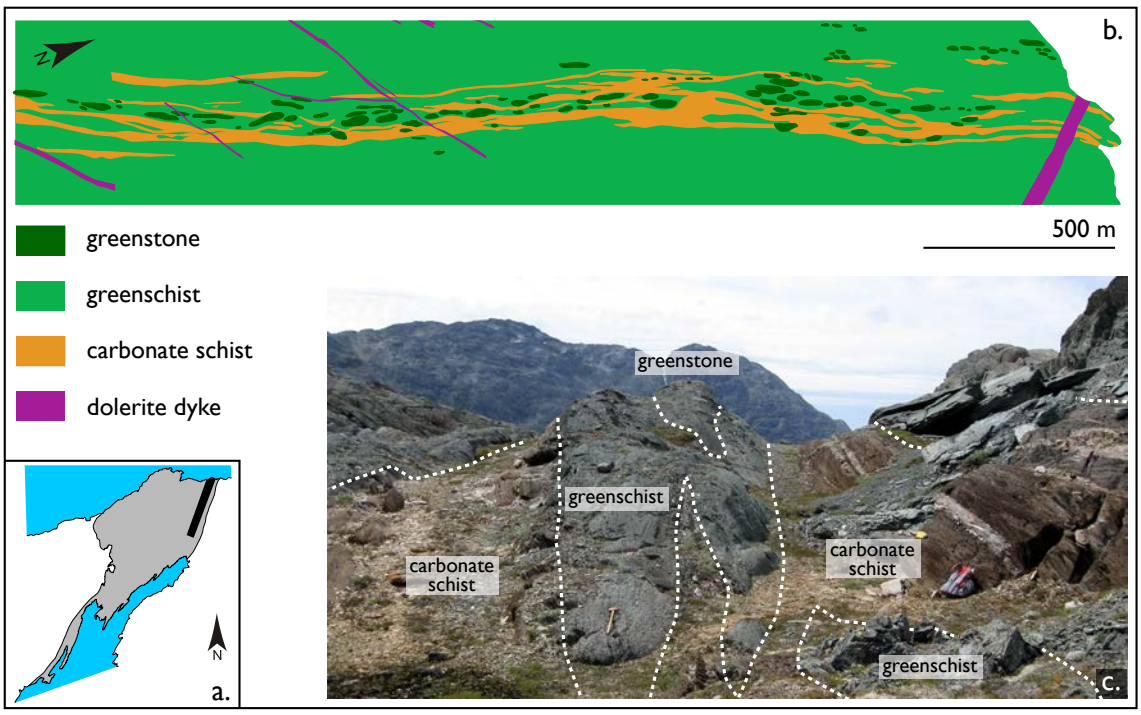

Figure 4. Simplified map (b) after Petersen (1992) of anastomosing network of greenschists and carbonate schists enclosing lenses of greenstone in eastern Nuuluk (a). A field photograph of this zone is shown in (c).

tion associated with this thrusting is intense and mylonitic textures are common. These felsic units are indistinguishable in mineralogy from those of the enclosing TTG gneisses, and further grade to an identical texture in the less deformed core regions. We, therefore, propose that these felsic layers represent slivers of TTG gneiss that were sliced off during thrusting and that subsequently accommodated the shear, developing into a mylonitic shearband at the base of the overriding Tartoq sheet. Thrusting is associated with folding, both on a large scale and as small buckling folds (see also Petersen 1992). The orientation of this thrusting is at an angle to the foliation that is incompatible with the foliation, which indicates that it does not represent the first phase of deformation (Petersen 1992). This angular relationship promotes the formation of the carbonate network in the knobbly greenschists.

High-grade mylonite thrusting is followed by an episode of extensive lower grade deformation, which produces cataclasite zones. In part, this overlaps in location with earlier mylonitic thrusting, with development of low-grade chlorite shear zones at the base of mylonite sheets (e.g. the western contact with the central gneiss in Sioralik, Fig. 2), but new deformation zones also develop. The cataclasite zones are characterised by a physical grinding up of the host rock, associated with introduction of chlorite. The size of fragments decreases from the host to the core of the deformation zone, and this produces a texture that resembles sedimentary grading (Fig. 3q). The introduction of chlorite is distinct, especially where these cataclasite zones are present within the TTG gneisses that are virtually devoid of primary ferromagnesian phases (e.g. west of Sioralik, Fig. 2). The brittle nature of the deformation and the secondary mineralogy that develops suggest deformation to have taken place at lower greenschist conditions, whereas the ductile behavior of both quartz and feldspar suggest temperature above 450°C for the mylonitic thrusting stage.

The contacts between Tartoq Group rocks and the enclosing TTG gneisses range from sharp, tectonic boundaries (e.g. the western contact of Iterlak and the eastern contact of Nuuluk) to a gradational transition consisting of a melange of TTG sheets and slivers of Tartoq (e.g. the western contacts of Nuuluk and Sioralik and the northern contact of Midternæs-N), as was also observed by Appel & Secher (1984) and Petersen (1991,1992). Intrusions of pegmatite sheets into the Tartoq Group are common for these gradational boundaries. With the exception of a clearly intrusive relationship in northern Midternæs-N, we interpret all contacts to be tectonic and related to the stacking of the TTGs and Tartoq rocks (a tectonic boundary may further be present north of the intrusive TTG in Midternæs-N). During this thrusting, the contacts are imbricated, which results on a small scale in the lenses of Tartoq rocks in the TTG gneisses at the block contacts (e.g. the western and eastern contacts of Iterlak and the southern contact of Sioralik), and on a large scale in the slivers of TTG at the base of thrust planes within the Tartoq blocks (e.g, the central felsic units in Nuuluk and Iterlak), and the cataclasite zones that form the western borders of Nuuluk and Sioralik. However, it cannot be excluded that these tectonic contacts overprint an original intrusive relationship between Tartoq Group rocks and the TTG gneisses.

A map showing the overall structural trends in the Tartoq Group is shown in Figure 5. Overall, we interpret the strike-slip domains as lateral ramps leading to the thrusting dominated blocks, and we extend this interpretation, originally proposed by Petersen (1992), to the Sioralik block and the lateral ramps of Midternæs-E.

A detailed analysis of microstructures, especially in relation to mineralisations, is presented in Petersen (1992) and Evans & King (1993).

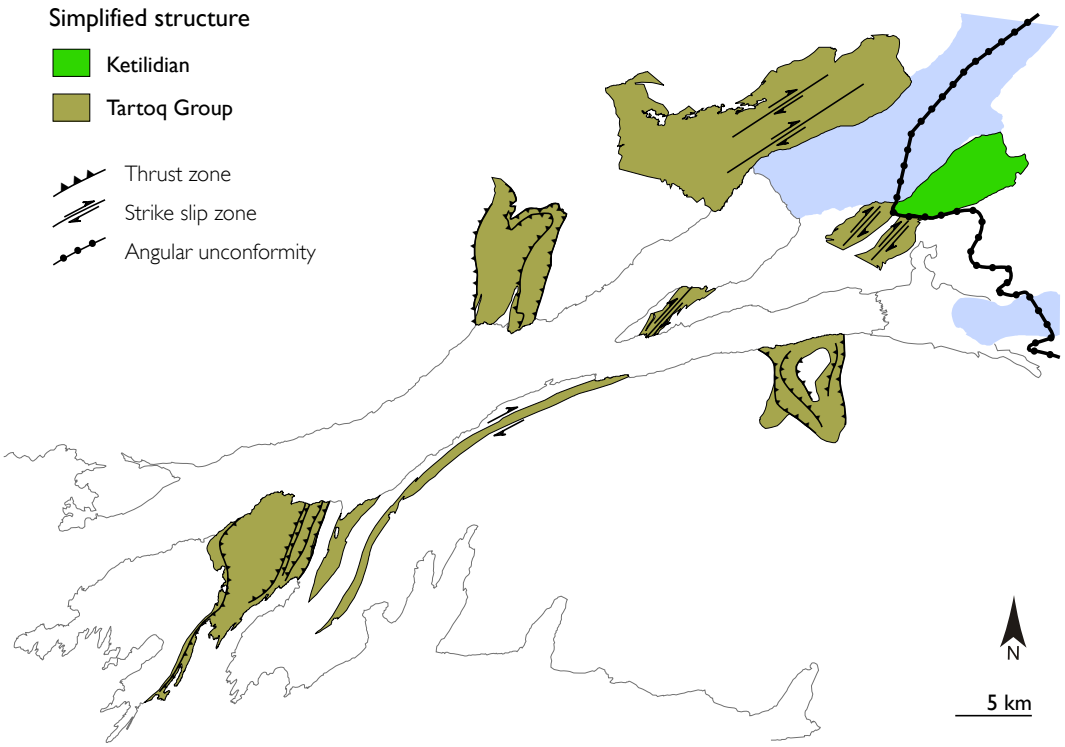

Figure 5. Overview map showing the main structures of the Tartoq Group along the Sermiligaarsuk Fjord (only areas visited during the 2009-2010 field campaign are shown).

History of the Tartoq Group rocks

Protoliths

The Tartoq supracrustals have been previously interpreted as a dominantly sedimentary succession with clastic and chemical sediments, mafic pyroclastics, felsic tuffs and mafic to felsic lava flows, which has been intruded by mafic sills and gabbro to ultramafic magma bodies (Higgins 1968, 1990; Berthelsen & Henriksen 1975; Appel & Secher 1984; King 1983, 1985; Petersen 1991, 1992; King & Evans 1993; Petersen & Madsen 1995). This interpretation was mainly derived from rock textures and structures. However, the strong imprint of metamorphism, deformation and hydrothermal activity on the Tartoq supracrustals complicates the assignment of textures to specific protoliths. For example, the cataclastic episode of deformation produces a texture that is, in outcrop, nearly identical to sedimentary graded bedding (Fig. 3q). Similarly, ductile deformation of greenschists in Nuuluk, associated with silicification, produces a laminated rock that strongly resembles a chert or even Banded Iron Formation (Fig. 3e).

The main structures and textures that have been reported for the Tartoq supracrustal rocks are briefly reviewed here:

1. *Sediments:* these include pyroclastics, Banded Iron Formations, carbonate and muscovite schists, a conglomerate, and felsic tuffs. With the exception of a Banded Iron Formation in Iterlak, with possible associated meta-sediments, we re-interpret the other

reported sediments as deformation or alteration related rocks. The pyroclastics are our knobbly greenschists, and, as already shown by Petersen (1991, 1992) and Evans & King (1993), their fragmented nature is not a primary feature, but results from deformation and associated carbonate influx, with subsequent carbonate dissolution producing irregular fragments of greenschist. These rocks are in fact so strongly overprinted that a protolith assignment cannot be made based on textures.

The felsic tuffs or acid volcanics (see King 1985; Petersen 1991, 1992; Evans & King 1993) describe the felsic sheets in between the mafic rocks of Nuuluk and Iterlak, and have further been used to describe muscovite-bearing rocks in, amongst others, Midternæs-E. In the case of the felsic sheets, we rather interpret these to represent slivers of TTG gneisses caught up in the thrusting and marking the base of thrust slices, as discussed above. Most of the other muscovite-bearing rocks are closely associated with carbonate schists, and both were originally interpreted as meta-sediments (Higgins 1968, 1990; Berthelsen & Henriksen 1975). However, replacement textures in thin sections, gradational contacts to enclosing greenschists and cross-cutting relationships have shown these to be an alteration product (King 1985, Evans & King 1993, Petersen 1992, this work). The prominent dolomite in Midternæs-N (Fig. 2) is similarly related to carbonation and a progressive increase in carbonate content can be observed that rips open the foliation of the greenschist protolith, eventually dominating the rock in fold hinges. This is not to say that primary felsic rocks and carbonates are absent in the Tartoq Group, but rather that caution should be applied and that the most obvious outcrops of felsic rocks and carbonate schists do not represent primary Tartoq components. In fact, the presence of felsic and calc-silicate layers in amphibolite in Sioralik (Figs. 3f,h), which as a block has seen negligible overprint, indicates that such units were indeed present, although their precise nature cannot readily be determined due to high grade metamorphism.

Widespread occurrence of Banded Iron Formations in Iterlak was reported by Appel & Secher (1984) and Petersen (1991, 1992), but detailed field observations during the 2010 field campaign indicate that most of these rather represent hydrothermal deposits consisting of two types; magnetite formed during serpentinisation of ultramafic lenses and subsequently segregated into alternating oxide and silicate bands during deformation (e.g. eastern Iterlak - Fig. 2, 3l), and sulfides introduced along large scale hydrothermal vein systems that crosscut all lithologies, including meta-gabbros (e.g. northern Iterlak - Fig. 2). Only in one locality did we observe a true Banded Iron Formation (Fig. 2 and detailed map of King 1985). This BIF consists of mm-thick layers of fine-grained magnetite alternating with silicate layers that are dominated by quartz (Fig. 3n). Despite being only a few mm thick, individual layers can be traced at constant thickness along the entire outcrop, whereas the layers in the metasomatic banded magnetite deposits are discontinuous on outcrop scale. Minor primary carbonate layers are also present in the BIF sequence. The Iterlak BIF is located next to the main hydrothermal vein network (see Fig. 2) and sulfides appear in the BIF closest to these veins. In fact, all "sulfide facies Banded Iron Formations" of Petersen (1991, 1992) can be shown to be secondary deposits that formed by replacement of primary Fe-minerals by introduction of S, a conclusion also reached by Evans & King (1993). A sedimentary magnetite-quartz unit in Nuuluk proposed by Petersen (1991, 1992) was observed to grade towards the east into a magnetite-rich greenstone, and more likely represents the deformed and altered equivalent of this unit (see also King 1985).

Although we did not visit the main conglomerate locality, photographs (pers. comm. A. Dziggel) and cataclastic textures observed elsewhere lead us to propose that this conglomerate could represent a cataclastic zone of deformation rather than a primary sedimentary deposit. However, more work is needed to confirm this. As it stands it is the only direct evidence for continent-derived sediments in the Tartoq Group.

2. Pillow structures: pillow structures in low-grade amphibolites and greenschists were reported on Nuna Qaqortoq (Higgins 1968), in Midternæs-N (Evans & King 1993) and in western Nuuluk (Petersen 1991). We did indeed observe lenticular structures in the Tartoq Group rocks that could be interpreted as pillows (Figs. 3r,s). However, we observed similar structures resulting from deformation, with shear bands enclosing less deformed lenses of precursor material. In the case of Nuna Qaqortoq, compositions of core and rim are strongly different, with rims being silicified suggesting element mobility in shear bands. However, these shear bands could exploit an original pillow derived contrast between core and rim. Although these localities are not conclusive, we favour a pillow origin at present, supported by observations of pillow structures in the southern part of Midternæs-N by A. Polat (pers. comm.) during this year's field season.

3. Flows and sills: lava flows and sills of mafic to felsic compositions are a primary component that is readily identified throughout the Tartoq Group. In Nuuluk, especially, these are present as competent sheets and lenses within the greenschist package (Figs. 3t,u). The deposits are variable in composition and mineralogy, which in some cases allows single sheets to be traced extensively, as in the case of a magnetite-rich sill that can be followed across the Nuuluk peninsula (Fig. 2). In thin section, relict grains of clino-pyroxene and plagioclase are common, as are ophitic textures. Sills and flows are affected by the later hydrothermal overprint, especially the transformation to knobbly greenschists, and they appear to form a major protolith component of the overall Tartoq package. Sills and dykes of intermediate compositions are also common and span a range of relative ages, although all have been affected by the hydrothermal stage (late-stage pegmatites and granites are excluded here). They commonly cross-cut and finger into the foliation (Fig 3v), although they have also been affected by deformation and folding.

4 Gabbroic and ultramafic intrusions: intrusives of mafic to ultramafic compositions are a second important protolith component to the Tartoq Group. Amphibolites with relict gabbroic textures are common in both Iterlak and Sioralik, and have also been observed as lenses in Midternæs-E. They range in composition from mafic to leucocratic and lenticular pods of leuco-gabbro have been observed in mafic gabbro in Iterlak suggestive of intrusive contacts. The ultramafic lenses of Sioralik, Midternæs-N and Nuna Qaqortoq are the best preserved, whereas these bodies have been extensively carbonated and sheared out in Iterlak and Midternæs-E. All ultramafic rocks have been serpentinised, but they preserve pseudomorphs after pyroxene, and in some cases a grain supported cumulate texture.

In conclusion, the dominant protoliths of the Tartoq Group supracrustals are mafic sills and lava flows, and gabbroic intrusions. These are complemented by surface deposits consisting of subaqueous mafic extrusives and minor marine chemical sediments, as well as ultramafic intrusions and/or cumulates. Volcanoclastics are a likely component in the sills/

flow sequence, but no evidence has been preserved, because these are most susceptible to overprinting. The compositions of these main components show a strong mid-ocean ridge affinity in both major and trace elements (Szilas, in prep.). We therefore interpret this package as a cross-section through Archaean oceanic crust from the deep, intrusion dominated subsurface to the ocean floor.

Metamorphism

Metamorphic conditions

The metamorphic grade of the rocks of the Tartoq Group spans a wide range from subgreenschist facies conditions in Nuuluk-E, to upper amphibolite to granulite facies conditions in Sioralik (Fig. 6). The former is characterised by fine-grained rocks dominated by chlorite and carbonate, with good preservation of bedding (Fig. 3w), whereas the latter shows breakdown of garnet and partial melting (Fig. 3f,g). The majority of Tartoq rocks have an intermediate grade ranging from greenschist to amphibolite facies conditions, characterised by a gradual transition from chlorite + plagioclase ± epidote ± actinolite, to chlorite + amphibole + plagioclase ± epidote, to amphibole + plagioclase, all with quartz and ilmenite, and commonly with carbonate. Ultramafic rocks contain an assemblage of magnetite + antigorite, and magnetite + antigorite + olivine in Sioralik, whereas felsic units consist of plagioclase + quartz + ilmenite ± K-feldspar ± muscovite ± biotite, all of which are consistent with grades from greenschist to amphibolite facies conditions.

Assessing the metamorphic conditions beyond these broad grade assignments is complicated owing to the rocks rarely recording a single equilibrium paragenesis or even bulk rock composition. Both relict primary mineral grains and hydrothermal overprint are common, with the latter associated with changes to bulk rock composition, mineralogy and mineral chemistry. Moreover, the effective bulk rock composition (i.e. the composition that takes part in mineral reactions) differs strongly from the measured bulk composition owing to sequestering of elements in non-reacting phases. For example, pyrrhotite and pyrite, which develop during hydrothermal activity (see above), sequester Fe, thereby strongly increasing the X_{Mg} of the remaining phases. Selective element incorporation by carbonates has a similar impact, although their composition and mineralogy evolve with grade. Because of these issues, mineral compositions cannot directly be used to constrain conditions.

Pseudosections (i.e. a *P-T* diagram for a specific bulk rock composition - Connolly 2005) are a more robust tool to constrain the *P-T* conditions for the Tartoq Group rocks, although care has to be taken to account for issues of effective bulk composition (see Evans 2004). We will, therefore, use them here only to constrain the *P-T* field of our samples. Figure 7 shows the pseudosection for a felsic schist from Nuuluk, calculated with the PerpleX suite of programs (Connolly 2005) for fluid saturated conditions (H_2O-CO_2 fluid with $X(CO_2) = 0.15$) and at the Ni-NiO fO_2 buffer. Chlorite-out, biotite-in, muscovite-out, K-feldspar-in and the onset of melting are the main changes in paragenesis as grade increases. Partial melting has not been observed, indicating that conditions for the TTG gneisses were below 700ºC throughout the Tartoq Group. Where a primary ferromagnesian phase is present in the felsic schists it is invariably biotite, although extensive retrogression to chlorite is commonly observed, especially in Nuuluk. Felsic schists in Nuuluk further contain muscovite, whereas this is absent from equivalent rocks in Iterlak and Sioralik. Together with the presence of K-feldspar, this constrains conditions for the Nuuluk felsic sheet (and hence mylonite formation) to a

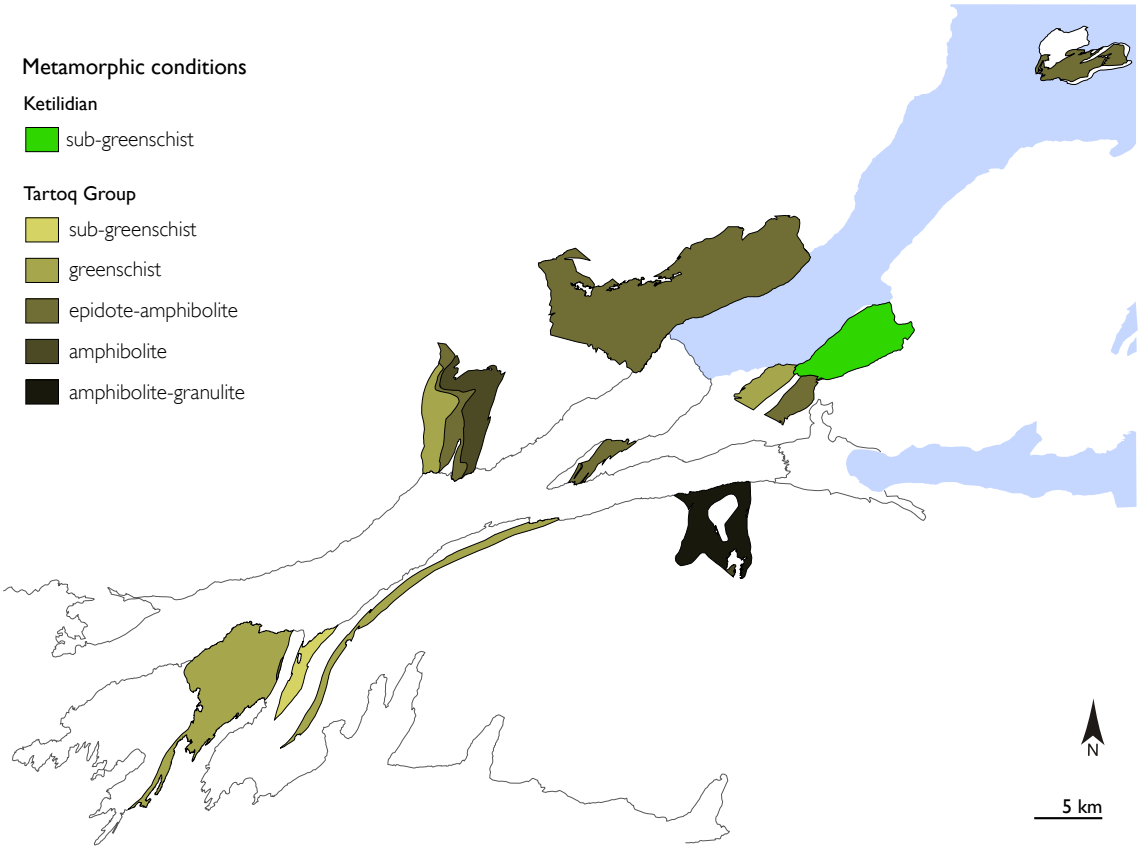

Figure 6. Overview metamorphic map of the Tartoq Group. Metamorphic grades are the dominant present-day grade for each domain. These represent mainly peak metamorphic conditions, but may include retrogression in areas strongly affected by hydrothermal overprint including central Nuuluk and the western valley of Iterlak. Only areas visited during the 2009-2010 field campaign are shown.

narrow band in *P-T* space (field 1 in Fig. 7). Conditions for the felsic sheets of Sioralik and Iterlak are beyond the muscovite-out isograd (field 2), but cannot be further constrained, because carbonates are not diagnostic in these rocks as they are directly controlled by the CO_3 content of the protolith.

The mafic rocks show a progressive change from chlorite to amphibole dominated parageneses with increasing grade, and appearance of garnet and development of partial melts at high temperature (Fig 8). The parageneses and position of field boundaries are strongly dependent on bulk rock composition for these mafic rocks as evident from the strong differences among the pseudosections in Figure 8. Combining field boundaries for a suite of samples of equal grade, but with different bulk compositions, and hence different parageneses, can therefore place tight constraints on *P-T* conditions. Figure 9 shows where the fields of coexisting parageneses overlap among the three pseudosections of Figure 8 for samples collected throughout the Tartoq Group. Lowest grade assemblages are characterised by chlorite + plagioclase + dolomite/calcite + quartz + ilmenite ± epidote. The lack of rutile and amphibole constrains the conditions for these assemblages to field 1. The early appearance of amphibole in some samples, and the presence of intercalated actinolite schists in the greenschists defines field 2, whereas fields 3 and 4 define the main amphibolite assemblages, with epidote + chlorite and without epidote + minor chlorite remaining, respectively. Garnet has not been observed except for several localities in Sioralik, which limits pressures for these fields to less than 6 kbar.

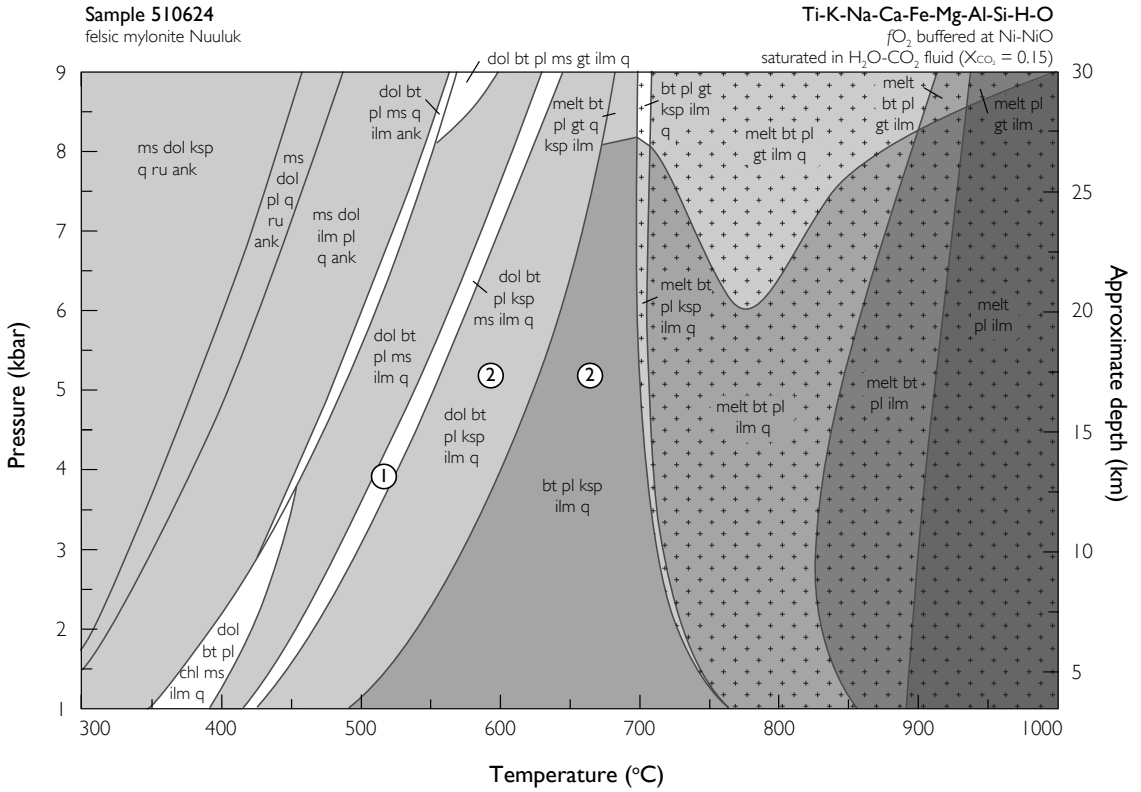

Figure 7. *P-T* pseudosection for a representative felsic mylonite from Nuuluk (sample 510866) calculated using the PerpleX suite of programs (Connolly 2005) in the Ti-K-Na-Ca-Fe-Mg-Al-Si-H-C-O chemical system and with the following mineral solid solution models as coded in solut_09.dat; Bio(TCC), Chl(HP), melt(HP), Ilm(WPH), Pl(h), OrFsp, Mica(CHA), and Gt(WPH). Bulk composition from Szilas (in prep.).

Rocks in Sioralik record the highest grades with the assemblage garnet + amphibole + plagioclase + quartz + ilmenite tightly constrained to field 5, mainly by the presence of quartz. The appearance of clino-pyroxene in this assemblage defines field 6, and partial melting, associated with the development of leucocratic rims on garnet (Figs. 3f,g), indicates that peak conditions exceeded the field boundary marked by 7 beyond which the garnet mode decreases. Further evidence for high temperatures in Sioralik compared to elsewhere in the Tartoq Group, is the presence of olivine in the ultramafic lenses and pseudomorphs after ortho-amphibole in one of these, which requires temperatures in excess of 550ºC (as determined from a pseudosection for this sample).

Petersen (1991) and Evans & King (1993) have proposed that the lower grade greenschist rocks of the Tartoq Group represent retrogression of amphibolites during hydrothermal activity, rather than peak metamorphic conditions. For the central part of Nuuluk and the western valley of Iterlak, this interpretation may well hold true, and relict grains of calcic amphibole rimmed by chlorite have been observed in several samples from these areas. Unfortunately, such relics are uncommon and retrogression appears to be near complete. For

► Figure 8. *P-T* pseudosections for three characteristic Tartoq mafic rock compositions calculated using the PerpleX suite of programs (Connolly 2005) in the Ti-Na-Ca-Fe-Mg-Al-Si-H-C-O chemical system and with the following mineral solid solution models as coded in solut_09.dat; Chl(HP), Amph(DPW), Ep(HP), oCcM(HP), Cpx(HP), melt(HP), Ilm(WPH), Pl(h), and Gt(WPH). Bulk rock compositions from Szilas (in prep.) Calculations were buffered at Ni-NiO oxygen fugacity and saturated in a H_2O-CO_2 fluid with a fixed X(CO_2) of 0.15.

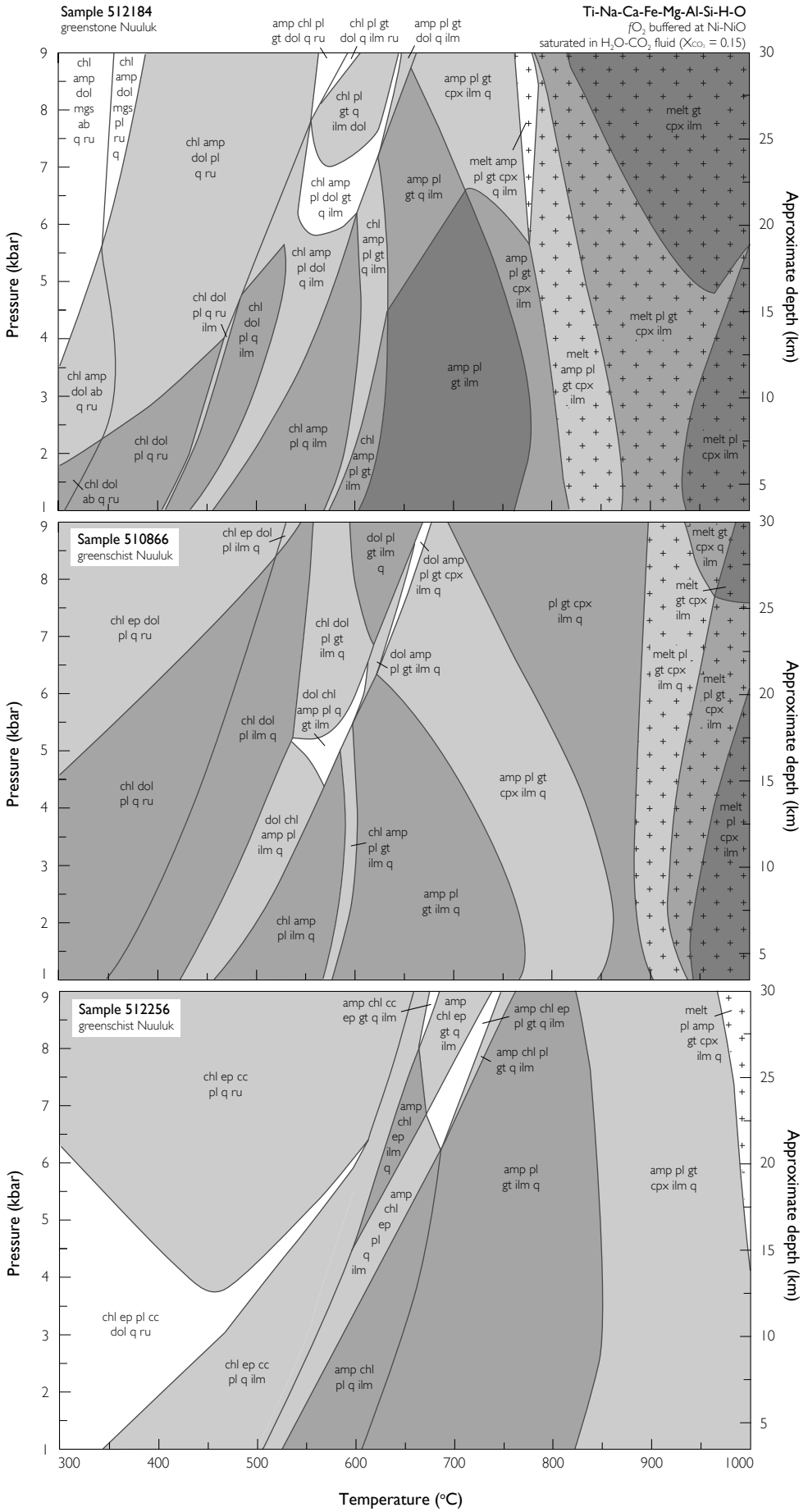
Sample 512184
greenstone Nuuluk
Ti-Na-Ca-Fe-Mg-Al-Si-H-O
fO_2 buffered at Ni-NiO
saturated in H_2O-CO_2 fluid (X_{CO_2} = 0.15)
amp chl pl gt dol q ru
chl pl gt dol q ilm ru
amp pl gt dol q ilm
chl amp dol mgs ab q ru
chl amp dol mgs pl ru q
chl amp dol pl q ru
chl pl gt q ilm dol
chl amp dol pl gt q ilm
amp pl gt q ilm
amp pl gt cpx ilm q
melt amp pl gt cpx q ilm
melt gt cpx ilm
chl amp pl gt q ilm
chl amp pl dol q ilm
chl dol pl q ru ilm
chl dol pl q ilm
amp pl gt cpx ilm
melt pl gt cpx ilm
melt amp pl gt cpx ilm
amp pl gt ilm
chl amp dol ab q ru
chl dol pl q ru
chl amp pl q ilm
chl amp pl gt ilm
chl dol ab q ru
melt pl cpx ilm
Sample 510866
greenschist Nuuluk
chl ep dol pl ilm q
dol pl gt ilm q
dol amp pl gt cpx ilm q
melt gt cpx q ilm
chl ep dol pl q ru
chl dol pl gt ilm q
pl gt cpx ilm q
melt gt cpx ilm
dol amp pl gt ilm q
melt pl gt cpx ilm q
dol chl amp pl q gt ilm
melt pl gt cpx ilm
chl dol pl ilm q
chl dol pl q ru
amp pl gt cpx ilm q
dol chl amp pl ilm q
chl amp pl gt ilm q
melt pl cpx ilm
amp pl gt ilm q
chl amp pl ilm q
Sample 512256
greenschist Nuuluk
amp chl cc ep gt q ilm
amp chl ep gt q ilm
amp chl ep pl gt q ilm
amp chl pl gt q ilm
melt pl amp gt cpx ilm q
chl ep cc pl q ru
amp chl ep ilm q
amp pl gt ilm q
amp pl gt cpx ilm q
amp chl ep pl q ilm
chl ep pl cc dol q ru
chl ep cc pl q ilm
amp chl pl q ilm
Pressure (kbar)
Approximate depth (km)
Temperature (°C)
1
2
3
4
5
6
7
8
9
5
10
15
20
25
30
300
400
500
600
700
800
900
1000

the eastern part of Nuuluk and the Tartoq slivers south of Sermiligaarsuk Fjord, hydrothermal overprint is much less of a concern and these rocks also display lower greenschist facies assemblages.

Tourmaline thermometry

Mineral thermometry further constrains the *P-T* conditions experienced by the Tartoq Group rocks, in particular tourmaline thermometry (see van Hinsberg & Schumacher 2007, 2009). Primary tourmaline is but a minor accessory in these rocks owing to the low primary boron content. However, it is one of the few phases that is resistant to the later hydrothermal overprint and does not re-equilibrate owing to negligible element diffusion rates. We have applied two tourmaline-based thermometers to these rocks; inter-sector thermometry (van Hinsberg & Schumacher 2007) and tourmaline-plagioclase Na-Ca exchange thermometry (van Hinsberg & Schumacher 2009).

Inter-sector thermometry is the more powerful technique, because it is based on element partitioning among sectors within a single tourmaline grain and avoids the need for equilibrium mineral assemblages, which are difficult to preserve. Moreover, sector zoning is destroyed upon re-equilibration, thereby providing an internal check, and various sector boundaries can be evaluated simultaneously to assess consistency of results (van Hinsberg & Schumacher 2007). Results for a greenschist from Nuuluk (sample 512169) give consistent temperatures of 370 ± 50 and 380 ± 50ºC for Ti and Ca derived temperatures, respectively, for 12 sector contacts.

Tourmaline-plagioclase thermometry was applied to this same sample using the temperature relation reported in van Hinsberg & Schumacher (2009). Results constrain the temperature to 380 ± 20ºC for 12 couples, and are in excellent agreement with results from inter-sector thermometry. Combining this temperature information with the pseudosection compilation shown in Figure 9, indicates that pressures were low during this greenschist metamorphism at less than 2 kbar.

Setting and timing of metamorphism

Rocks of the Tartoq Group record a remarkably extensive range of metamorphic conditions from sub-greenschist facies conditions at low pressure, to partial melting at 850ºC and pressures that exceed 6 kbar. These grades are, furthermore, relatively constant within blocks and where multiple grades are present, these are separated by thrusts (e.g. Iterlak - Fig. 6) and change step-wise. This lack of metamorphic gradients indicates that metamorphism predates the stacking of the Tartoq blocks, and, therefore, must have taken place elsewhere. Grades further exceed those observed in the TTG gneisses, both for those within and directly enclosing the Tartoq Group, which shows that metamorphism of the TTG gneisses is independent of Tartoq Group metamorphism. The same is true for a comparison with the regional metamorphic grade determined from mafic and ultramafic rocks of the basement (Schumacher *et al.* 2011). In fact, extensive migmatisation should have been observed for TTGs enclosing Sioralik if metamorphism had been contemporaneous. Age constraints agree with this interpretation, with ages for mafic Tartoq rocks predating the enclosing TTGs by up to 200 Ma (Szilas, in prep.).

The ocean floor setting in which these rocks formed, see above, would be the first environment where metamorphism would develop, induced by strong hydration owing to the circu-

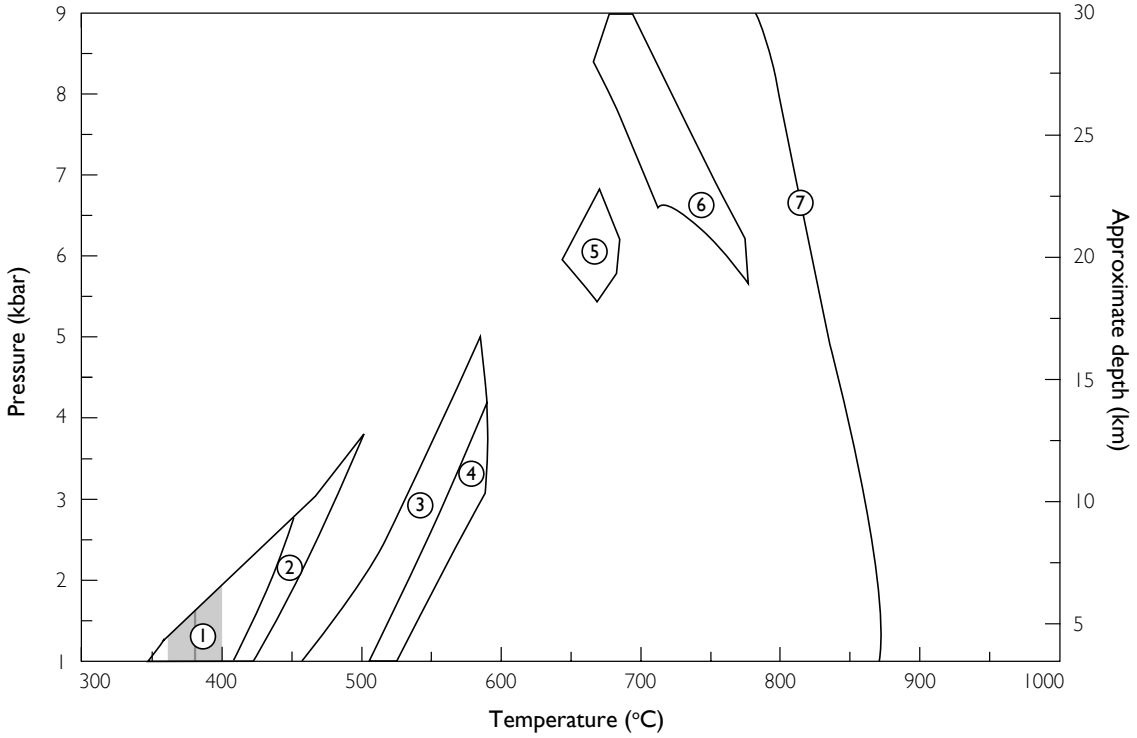

Figure 9. Compilation of *P-T* field constraints from the intersection of coexisting mineral assemblages among the three pseudosections of Figure 8. Grade increases from field 1 to the development of partial melting and leucocratic rims on garnet, which requires crossing field boundary 7. Tourmaline thermometry results are shown by the gray line with its associated 1 sigma uncertainty.

lation of ocean water derived hydrothermal fluids. The extent of this metamorphism is controlled directly by the access of fluids to these rocks, which in turn is strongly controlled by the stress field and deformation style of the new-formed oceanic crust. The lack of sheeted dykes in an otherwise oceanic ridge style crust sequence, here and in many Archaean ocean crust sections worldwide, has been taken to indicate rapid extension and a weak crust in which the brittle fractures needed for dyke emplacement do not form (Dilek & Polat 2008). This scenario would hinder access of fluids, and hence limit this initial metamorphism to shallow levels of the crust.

The main component that would be missing in an in-situ ocean crust metamorphism scenario is deformation. In contrast, amphibolites in Sioralik and Iterlak, which have been minimally affected by later overprint, show gneissic banding and extensive deformation that is syn-metamorphic (Fig. 3h). Partial melt migration is, furthermore, syn-tectonic (Fig. 3g). We therefore conclude that peak metamorphism could not have developed in a static ocean floor setting, but took place in a tectonic environment and likely during an early stage of convergence. Our present working hypothesis is that metamorphism and deformation took place in a subduction setting, with the Tartoq Group part of the subducting plate. However, the relatively low pressures indicate that the Tartoq Group was rapidly severed from the downgoing slab, possibly due to emplacement of TTG melts giving it buoyancy (e.g. the intrusive TTG of Midternæs-N - Fig. 2). Subsequent exhumation in the subduction channel would lead to imbrication with TTG gneisses of the overriding plate. The early mylonitic and later cataclastic styles of deformation associated with this imbrication indicate that this took place in two stages.

Hydrothermal overprint

Hydrothermal overprint of the rocks of the Tartoq Group commences with an episode of extensive carbonation that is intimately linked to thrusting tectonics. This link is evidenced especially by the close association of talc-carbonate schists and thrust planes in eastern Iterlak, Midternæs-E and Sioralik. Here, introduction of carbonate-rich fluids to the ultramafic lenses produces an assemblage of talc, magnetite and carbonate that is subsequently smeared out to line the thrust planes. Establishing the conditions for this assemblage is difficult, because it depends strongly on the $X(CO_2)$ in the carbonating fluid. However, the lack of antigorite in the talc schist puts the $X(CO_2)$ in excess of 0.04 (as determined from pseudosections for these rocks), which in turn suggests temperatures were above 450ºC. Further evidence for a close link between thrusting and hydrothermal activity is the Nuuluk Linear Belt. This belt in central Nuuluk, which is parallel to the thrust planes, displays the strongest overall hydrothermal overprint, and this intensifies even further in the foot wall of the three thrust zones that have been recognized within it (the "Eastern and Western Carbonate Zones", and "Felsic Tuff Zone" of Petersen 1991 - Fig. 2).

Tourmaline is also associated with this initial stage of hydrothermal activity and small idiomorphic grains of tourmaline develop throughout the greenschists of Nuuluk and Iterlak. The colour of these grains varies from brown to pale blue depending on the bulk rock composition of their host, and this, together with a lack of correlation between tourmaline mode and bulk rock composition indicates that tourmaline resulted from external input of boron. The combination of BO_3 and CO_3 in the hydrothermal fluids suggests that they are of ocean water origin, and that this event may represent an ocean floor style alteration. However, this environment cannot be the original depositional environment, as the rocks were metamorphosed and deformed prior to this hydrothermal activity, and this fluid signature may rather represent release of fluids from a lithology that was previously altered by ocean water.

Subsequent activity is channelized into anastomosing networks, and dominated by the formation of ankerite schists from greenschists. This carbonation is accompanied by metasomatism of vein walls, as evidenced by the abundant appearance of fuchsite that develops as a result of residual enrichment in Cr. Boundaries between greenschists and carbonate schists are remarkably sharp, especially in eastern Nuuluk (see Petersen 1992), which led earlier studies to conclude that these are a primary lithology rather than an alteration product (e.g. Appel and Secher 1984). However, in thin section, the rocks are clearly an alteration product with ankerite replacing Fe-oxides (see also Evans & King 1993), and they locally crosscut lithology boundaries (King 1985). Still, a primary compositional contrast between the greenschists and the carbonate schist protolith, as proposed by Petersen (1992), cannot be excluded. Conditions for this stage have not yet been determined. The carbonate schists and the carbonate-greenschist contacts are commonly folded and crenulated, which indicates that this episode was followed by renewed deformation. According to Petersen (1992) this deformation is parallel to the deformation resulting from thrusting along the internal thrust zones.

The final episode of hydrothermal activity is characterised by deposition of sulfides, including pyrite, pyrrhotite and arsenopyrite (Appel and Secher 1984; Petersen 1992; Evans and King 1993). Activity is closely associated with the thrust zones, and foot wall rocks are extensively altered (e.g. Fig. 3o), showing silicification and local appearance of graphite. The presence of graphite and sulfides indicates that the fluids responsible for alteration were reducing in nature. A second generation of hydrothermal tourmaline also develops with

mutual overgrowth relations between sulfide and tourmaline. Preliminary results for a single tourmaline grain from a greenschist directly in the thrust zone (sample 512281) suggest temperatures were up to 500ºC, which is substantially higher than the peak metamorphic temperature for the surrounding greenschists. Temperatures from arsenopyrite thermometry are somewhat lower at 350-450ºC (Evans & King 1993). Aside from the association with thrust zones, sulfides are concentrated on Fe-rich protolith lithologies, including Banded Iron Formations, magnetite-rich sills and magnetite-talc schists. We propose that the ankerite-quartz veins in the central parts of carbonate schists (e.g. Fig. 3p) also form during this episode of activity. Interestingly, sulfides in these deposits have been cataclastically deformed with chlorite forming on fracture surfaces (Evans & King 1993), suggesting a possible link between this episode of hydrothermal activity and the formation of cataclasite zones throughout the Tartoq Group.

The gold associated with the hydrothermal overprint of the Tartoq rocks is concentrated in the sulfide rich horizons, but elevated gold contents are observed throughout (Geisler 1972, 1975; King 1983, 1985; Appel & Secher 1984; Petersen 1991, 1992; Evans & King 1993). This suggests that gold was introduced during the early stages of pervasive alteration and subsequently remobilised and concentrated (Evans & King 1993; Petersen & Madsen 1995). The close association with sulfide-rich horizons, which themselves represent sulfidisation of Fe-rich protoliths suggests that deposition is controlled by local geochemical traps, possibly in a process of gold mobility in Au-bisulfide complexes that are destabilised by reaction with Fe-oxides to form sulfides.

Conclusions

The results presented here provide a preliminary overview of the Tartoq Group supracrustal rocks, and their history from protolith through metamorphism to hydrothermal overprint. More work is on the way to better constrain the *P-T-X* conditions experienced during the different stages of its formation, based on samples collected in the 2010 field season and more detailed petrological and mineral chemistry work.

At present, our best understanding of these rocks suggests an oceanic crust protolith for the Tartoq Group with deposits ranging from deep gabbroic to ultramafic intrusives, to mafic flows, sills and volcanoclastics, to (chemical) sediments deposited on the ocean floor. This sequence was probably subjected to alteration on the ocean floor by ocean water derived hydrothermal fluids, but the main stage of metamorphism took place in a tectonically active zone, leading to development of a penetrative foliation, gneissic banding and extensive isoclinal folding. Peak metamorphic grades span a remarkably large range from sub-greenschist facies conditions to the onset of melting at temperatures in excess of 850ºC, and we envision a shallow subduction setting as the environment for metamorphism. This metamorphism takes place before thrusting and imbrication of Tartoq rocks and TTG gneisses, which appears to uniformly take place at conditions of ca. 450ºC and leads to development of mylonite zones. We propose that this imbrication takes place during exhumation of the Tartoq Group in a subduction channel. Deformation continues beyond this initial thrusting as evidenced in folding of thrust planes and the development of greenschist facies cataclasite zones. Extensive hydrothermal activity overprints the earlier metamorphic parageneses and textures, but is intimately associated with thrusting. Activity commences with pervasive fluid

infiltration of CO_2 and BO_3 rich fluids, and progresses to more and more channelized flow in an anastomosing network. The thrust planes also act as conduits for hydrothermal fluids with extensive alteration of foot walls, culminating in the formation of graphite-sulfide bearing "black shales" and enrichment of gold up to economic levels in sulfide rich horizons. The setting of hydrothermal activity for these three stages has not been constrained, but the carbonate and borate rich nature of the initial stage suggests involvement of ocean water derived fluids, followed by a stage of chemically distinct, S-bearing low fO_2 fluids.

Acknowledgements

This report is based on GEUS-led fieldwork conducted in the summers of 2009 and 2010, and we thank our field partners Brian Windley, Denis Schlatter, Kirsty Reynolds, Ali Polat and Anika Dziggel for their help in the field, and comments and suggestions during our enjoyable evening discussions on the Tartoq Group. We thank the base camp staff, Jakob, Klaus and Marianne, in particular, for their excellent care during our stay in the field, and BMP and GEUS for funding. Further details of this fieldwork, and locations of observations and samples can be found in our field notes deposited with GEUS.

References

Appel, P.W.U. & Secher, K. 1984: On a gold mineralization in the Precambrian Tartoq Group, SW Greenland. Journal of the Geological Society 141, 273-278

Berthelsen, A. & Henriksen, N., 1975: Geological map of Greenland, 1:100000, Ivigtut, 61 VI. Syd. Meddelelser om Gronland 186, 169 pp.

Connolly, J. A. D., 2005: Computation of phase equilibria by linear programming: a tool for geodynamic modelling and its application to subduction zone decarbonation. Earth and Planetary Science Letters 236, 524–541.

Dilek, Y. & Polat, A., 2008: Suprasubduction zone ophiolites and Archean tectonics. Geology 36, 431-432.

Escher, J.C. & Jensen, S.B. 1974: Geological map of Greenland with English legend, 1: 100 000, 61 V.2 Nord, Midternæs.

Evans, T. P., 2004: A method for calculating effective bulk composition modification due to crystal fractionation in garnet-bearing schist: implications for isopleth thermobarometry. Journal of Metamorphic Geology 22, 547–557.

Evans, D.M. & King, A.R. 1993: Sediment and shear-hosted gold mineralization of the Tartoq Group supracrustals, southwest Greenland. Precambrium Research 62, 61-82.

Garde, A.A., Chadwick, B., McCaffrey, K. & Curtis, M. 1998: Reassessment of the north-western border zone of the Palaeoproterozoic Ketilidian orogen, South Greenland. Geology of Greenland Survey Bulletin 180, 111-118.

Geisler, R.A. 1972: Investigations on the Renzy Mines Limited Frederikshaab concession, Greenland, to June 15, 1972. Renzy Mines Limited 74 pp.

Geisler, R.A. 1975: Investigations on the Frederikshaab exploration concession of Renzy Mines Ltd. During the year ended June 15, 1975. Renzy Mines Limited 32 pp.

Henriksen, N. 1968: Geological map of Greenland with English legend, 1: 100 000, 61 V.1 Syd, Ivigtut.

Higgins, A.K. 1968: The Tartoq Group on Nuna Qaqortoq and in the Iterdlak area, South-West Greenland. Grønlands Geologiske Undersøgelse 17, 17 pp.

Higgins, A.K. 1990: Descriptive text to 1:100 000 sheets Neria 61 V.1 N and Midternæs 61 V.2 N. Grønlands Geologiske Undersøgelse, 23 p.

Jensen, S.B. 1975: Geological map of Greenland with English legend, 1: 100 000, 61 V.1 Nord, Neria.

King, A.R. 1983: Greenex A/S Frederikshaab prospecting license. Report on sampling and prospecting in the Sermiligarssuk Fjord area, South-west Greenland. Greenex A/S, 46pp.

King, A.R. 1985: Greenex A/S Sermiligarssuk exploration concession. Report on geological field work carried out in the Sermiligarssuk Fjord area, South-west Greenland, July-August 1984. Greenex A/S 142 pp.

Nutman, A.P. & Kalsbeek, F. 1994: A minimum age of 2944 ± 7 Ma for the Tartoq Group, South-West Greenland. Rapport Grønlands Geologiske Undersøgelse 161, 35-38.

Petersen, J.S. 1991: Gold mineralization in the Taartoq Group greenstones, SW Greenland - results of structural, geochemical and geophysical exploration studies: Nuuk, Nunaoil A/S. 59pp.

Petersen, J.S. 1992: Nuuluk-Iterlak gold and massive-sulfide project, Taartoq Archaean greenstone belt, SW Greenland. Field report. Nuuk, NunaOil A/S. 164 pp.

Petersen, J.S. & Madsen, A.L. 1995: Shear-zone hosted gold in the Archaean Taartoq greenstone belt, South-west Greenland. In Ihlen, P.M., Pedersen, M. & Stendal, H. (Eds.) Gold mineralization in the Nordic countries and Greenland. Extended abstracts and field trip guide, 95/10: Copenhagen, Open File Series Grønlands Geologiske Undersøgelse, 65-68.

Steenfelt, A. 2000: Geochemical signatures of gold provinces in South Greenland. Transactions of the Institution of Mining and Metallurgy, Section B - Applied Earth Science 109, B14-B22.

van Hinsberg V.J. & Schumacher J.C., 2007: Intersector element partitioning in tourmaline; a powerful single crystal thermometer. Contributions to Mineralogy and Petrology 153, 289-301.

van Hinsberg V.J. & Schumacher J.C. 2009: The geothermobarometric potential of tourmaline, based on experimental and natural data. American Mineralogist 94, 761-770.

Appendix 1. Selected back-scattered electron images of samples

Sample 512169. Central Nuuluk laminated greenschist.

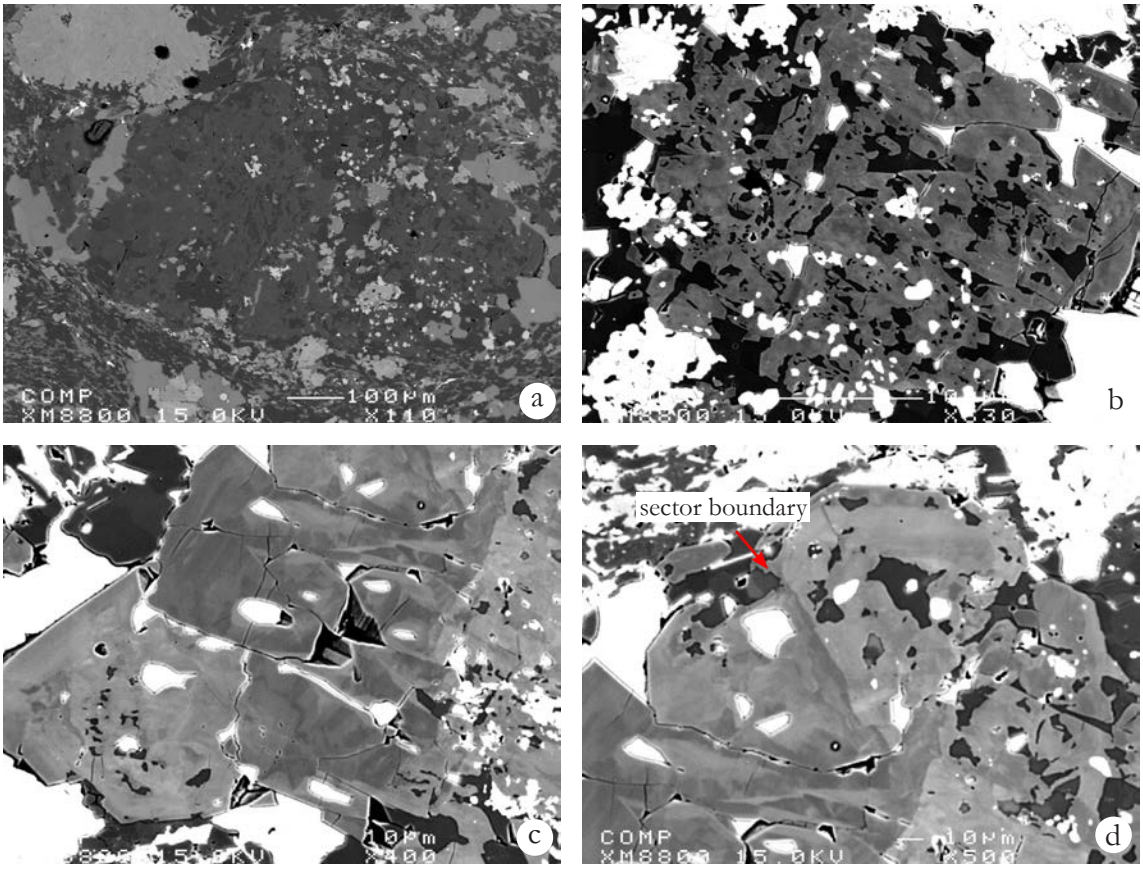

Figure A1.1. Overview of metamorphic tourmaline cluster intergrown with the metamorphic mineral assemblage (a,b); detailed views of compositional zoning in tourmaline (c-d) showing sector zoning crosscutting the concentric growth zoning.

Sample 512181. Central Nuuluk laminated greenschist in thrust zone with associated sulfide mineralisation.

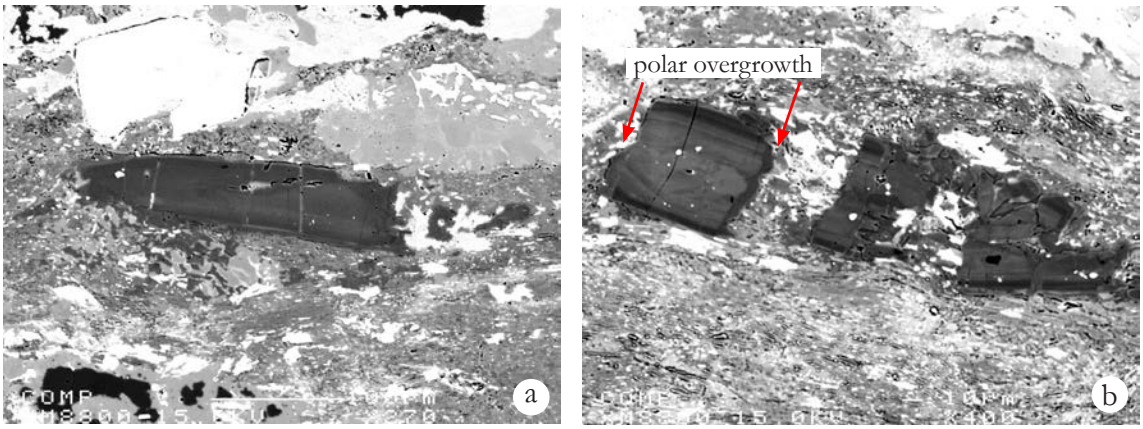

Figure A1.2. Metamorphic tourmaline grains with their long axis aligned to the foliation. Both grains have a tourmaline overgrowth rim related to hydrothermal activity. The grain in (b) has been fractured and pulled apart and overgrowths are present on both sides of the fracture with polar compositional differences.

Appendix 2. Electron microprobe data for Tartoq samples

Sample 512169. Central Nuuluk laminated greenschist.

sample code	169-1	169-2	169-3	169-4	169-5	169-6	169-7	169-8	169-9	169-10
mineral	tour	tour	tour	tour	tour	tour	tour	tour	tour	tour
SiO_2	36.71	36.97	36.28	36.81	36.52	36.91	37.01	36.38	37.29	36.79
TiO_2	0.40	0.09	0.34	0.38	0.60	0.32	0.22	0.45	0.08	0.39
Al_2O_3	30.49	32.88	30.02	31.16	30.18	30.94	32.40	31.16	32.95	31.21
Cr_2O_3	< d.l.	0.02	< d.l.	< d.l.	0.02	0.01	0.01	< d.l.	0.01	0.01
MgO	7.14	6.83	7.42	7.29	7.37	7.72	6.75	6.83	7.05	7.25
MnO	0.04	0.02	0.01	0.04	0.04	0.04	< d.l.	0.03	0.05	0.02
FeO	8.36	6.71	8.55	7.56	8.12	7.11	7.02	8.47	6.41	7.43
CaO	0.75	0.40	0.99	0.48	1.23	0.52	0.37	0.75	0.32	0.67
Na_2O	2.18	1.78	2.13	2.18	2.09	2.22	1.82	2.11	1.90	2.16
K_2O	0.01	0.00	0.01	0.01	0.02	0.01	0.01	0.01	0.00	0.00
F	0.11	0.04	0.08	0.12	0.04	0.18	< d.l.	0.14	< d.l.	0.20

Cations per formula unit based on: for tourmaline a Y+Z+T = 15 normalization scheme (assuming no vacancies or B in the Y, Z or T sites); to 5 cations for plagioclase; to 1 cation for rutile; to 10 cations for chlorite; and to 8 cations for epidote.

Si	6.08	6.05	6.04	6.06	6.06	6.08	6.08	6.01	6.07	6.07
Ti	0.05	0.01	0.04	0.05	0.08	0.04	0.03	0.06	0.01	0.05
Cr	5.95	6.34	5.89	6.05	5.90	6.00	6.27	6.07	6.32	6.07
Al	< d.l.	0.00	< d.l.	< d.l.	0.00	0.00	0.00	< d.l.	0.00	0.00
Mg	1.76	1.67	1.84	1.79	1.82	1.89	1.65	1.68	1.71	1.78
Mn	0.01	0.00	0.00	0.00	0.01	0.01	< d.l.	0.00	0.01	0.00
Fe	1.16	0.92	1.19	1.04	1.13	0.98	0.96	1.17	0.87	1.03
Ca	0.13	0.07	0.18	0.09	0.22	0.09	0.06	0.13	0.06	0.12
Na	0.70	0.57	0.69	0.70	0.67	0.71	0.58	0.68	0.60	0.69
K	0.00	0.00	0.00	0.00	0.00	0.00	0.00	0.00	0.00	0.00
F	0.06	0.02	0.04	0.06	0.02	0.10	< d.l.	0.07	< d.l.	0.10

Appendix 2. Continued

Sample 512169. Central Nuuluk laminated greenschist.

sample code	169-11	169-12	169-13	169-14	169-15	169-16	169-20	169-21	169-22	169-23
mineral	tour	tour	tour	tour	tour	tour	tour	tour	tour	tour
SiO_2	36.78	36.41	36.87	36.64	37.47	36.85	36.60	36.77	35.92	35.80
TiO_2	0.26	0.54	0.08	0.34	0.09	0.44	0.16	0.15	0.52	0.20
Al_2O_3	30.85	30.03	33.21	30.88	32.74	30.58	32.36	31.75	29.52	31.51
Cr_2O_3	< d.l.	0.04	< d.l.	0.01	0.01	< d.l.	0.01	0.02	0.02	< d.l.
MgO	7.59	7.50	6.97	7.01	6.96	7.13	6.79	7.16	7.40	7.05
MnO	0.04	0.06	0.01	0.03	0.02	0.04	< d.l.	0.02	0.02	0.05
FeO	7.57	8.17	6.39	7.94	6.65	8.63	6.69	6.78	8.09	6.72
CaO	0.58	1.11	0.17	0.51	0.21	0.64	0.36	0.54	1.13	0.55
Na_2O	2.20	2.09	1.80	2.17	1.85	2.23	1.82	1.92	2.09	1.89
K_2O	0.00	0.01	0.00	0.00	0.00	0.01	0.00	0.01	0.02	0.01
F	0.14	0.08	< d.l.	0.18	< d.l.	0.14	0.08	0.04	0.08	0.04

Cations per formula unit based on: for tourmaline a Y+Z+T = 15 normalization scheme (assuming no vacancies or B in the Y, Z or T sites); to 5 cations for plagioclase; to 1 cation for rutile; to 10 cations for chlorite; and to 8 cations for epidote.

Si	6.06	6.05	6.02	6.08	6.10	6.07	6.06	6.08	6.06	6.02
Ti	0.03	0.07	0.01	0.04	0.01	0.05	0.02	0.02	0.07	0.02
Cr	5.99	5.88	6.39	6.04	6.29	5.93	6.32	6.19	5.87	6.24
Al	< d.l.	0.00	< d.l.	0.00	0.00	< d.l.	0.00	0.00	0.00	< d.l.
Mg	1.86	1.86	1.70	1.73	1.69	1.75	1.68	1.77	1.86	1.77
Mn	0.01	0.01	0.00	0.00	0.00	0.01	< d.l.	0.00	0.00	0.01
Fe	1.04	1.13	0.87	1.10	0.91	1.19	0.93	0.94	1.14	0.94
Ca	0.10	0.20	0.03	0.09	0.04	0.11	0.06	0.10	0.20	0.10
Na	0.70	0.67	0.57	0.70	0.58	0.71	0.58	0.62	0.68	0.62
K	0.00	0.00	0.00	0.00	0.00	0.00	0.00	0.00	0.00	0.00
F	0.07	0.04	< d.l.	0.09	< d.l.	0.07	0.04	0.02	0.04	0.02

Appendix 2. Continued

Sample 512169. Central Nuuluk laminated greenschist.

sample code	169-24	169-25	169-26	169-27	169-28	169-29	169-30	169-31	169-32	169-33
mineral	tour	tour	tour	tour	tour	tour	tour	tour	tour	tour
SiO_2	36.19	36.26	36.38	35.97	36.10	35.38	36.55	36.14	36.23	35.66
TiO_2	0.46	0.28	0.09	0.49	0.14	0.50	0.05	0.50	0.24	0.46
Al_2O_3	29.63	30.94	31.89	30.75	31.81	30.30	32.03	29.77	31.09	29.58
Cr_2O_3	0.04	0.06	0.04	0.09	0.04	0.10	0.03	0.10	0.03	0.03
MgO	7.40	7.30	7.16	7.18	7.13	7.21	7.07	7.33	7.33	7.40
MnO	0.03	0.02	0.02	0.01	< d.l.	0.01	0.03	0.06	0.01	0.04
FeO	8.38	7.11	6.68	7.59	6.73	7.80	6.67	7.97	6.81	7.88
CaO	1.07	0.91	0.25	1.15	0.24	1.12	0.23	1.11	0.37	1.17
Na_2O	2.05	2.15	2.01	2.06	2.09	2.07	1.98	2.05	2.07	2.15
K_2O	0.00	0.01	0.01	0.02	0.00	0.01	0.00	0.01	0.01	0.02
F	0.08	0.03	0.03	< d.l.	0.06	0.03	0.06	0.02	0.08	0.07

Cations per formula unit based on: for tourmaline a Y+Z+T = 15 normalization scheme (assuming no vacancies or B in the Y, Z or T sites); to 5 cations for plagioclase; to 1 cation for rutile; to 10 cations for chlorite; and to 8 cations for epidote.

Si	6.06	6.05	6.04	6.01	6.02	5.97	6.06	6.07	6.06	6.04
Ti	0.06	0.04	0.01	0.06	0.02	0.06	0.01	0.06	0.03	0.06
Cr	5.85	6.09	6.24	6.06	6.25	6.03	6.26	5.89	6.13	5.91
Al	0.01	0.01	0.01	0.01	0.00	0.01	0.00	0.01	0.00	0.00
Mg	1.85	1.82	1.77	1.79	1.77	1.82	1.75	1.83	1.83	1.87
Mn	0.00	0.00	0.00	0.00	< d.l.	0.00	0.00	0.01	0.00	0.01
Fe	1.17	0.99	0.93	1.06	0.94	1.10	0.92	1.12	0.95	1.12
Ca	0.19	0.16	0.05	0.21	0.04	0.20	0.04	0.20	0.07	0.21
Na	0.67	0.70	0.65	0.67	0.68	0.68	0.64	0.67	0.67	0.71
K	0.00	0.00	0.00	0.00	0.00	0.00	0.00	0.00	0.00	0.00
F	0.04	0.02	0.02	< d.l.	0.03	0.02	0.03	0.01	0.04	0.04

Appendix 2. Continued

Sample 512169. Central Nuuluk laminated greenschist.

sample code	169-35	169-36	169-37	169-38	169-p2	169-p3	169-p4	169-p5	169-p6	169-p7
mineral	tour	tour	tour	tour	plag	plag	chl	chl	chl	ep
SiO_2	36.10	36.14	35.84	36.04	67.02	67.95	25.25	25.18	25.58	37.24
TiO_2	0.48	0.27	0.70	0.24	0.01	0.01	0.04	0.19	0.06	0.12
Al_2O_3	29.70	30.61	29.31	31.24	21.72	21.14	22.36	21.71	21.82	24.00
Cr_2O_3	0.09	< d.l.	0.08	< d.l.	< d.l.	< d.l.	0.07	0.06	0.03	< d.l.
MgO	7.33	7.32	7.32	7.12	< d.l.	< d.l.	17.03	17.76	17.40	0.02
MnO	0.04	0.05	0.04	0.03	0.02	< d.l.	0.24	0.24	0.26	0.34
FeO	7.83	7.27	8.30	7.37	0.25	0.27	21.13	20.41	20.29	10.57
CaO	1.10	0.53	1.46	0.37	0.52	0.47	0.10	0.11	0.22	22.93
Na_2O	2.13	2.09	1.81	2.04	11.21	11.21	0.02	< d.l.	0.04	0.01
K_2O	0.01	0.01	0.02	0.00	0.01	0.00	0.00	0.00	0.00	0.00
F	0.07	0.11	0.12	0.05	< d.l.	< d.l.	0.06	0.03	0.02	< d.l.

Cations per formula unit based on: for tourmaline a Y+Z+T = 15 normalization scheme (assuming no vacancies or B in the Y, Z or T sites); to 5 cations for plagioclase; to 1 cation for rutile; to 10 cations for chlorite; and to 8 cations for epidote.

Si	6.08	6.06	6.05	6.02	2.91	2.95	2.66	2.66	2.70	3.00
Ti	0.06	0.03	0.09	0.03	0.00	0.00	0.00	0.01	0.00	0.01
Cr	5.90	6.05	5.83	6.15	1.11	1.08	2.77	2.70	2.71	2.28
Al	0.01	< d.l.	0.01	< d.l.	< d.l.	< d.l.	0.01	0.01	0.00	< d.l.
Mg	1.84	1.83	1.84	1.77	< d.l.	< d.l.	2.67	2.79	2.74	0.00
Mn	0.00	0.01	0.01	0.00	0.00	< d.l.	0.02	0.02	0.02	0.02
Fe	1.10	1.02	1.17	1.03	0.01	0.01	1.86	1.80	1.79	0.71
Ca	0.20	0.10	0.26	0.07	0.02	0.02	0.01	0.01	0.02	1.98
Na	0.70	0.68	0.59	0.66	0.94	0.94	0.00	< d.l.	0.01	0.00
K	0.00	0.00	0.00	0.00	0.00	0.00	0.00	0.00	0.00	0.00
F	0.04	0.06	0.06	0.03	< d.l.	< d.l.	0.02	0.01	0.01	< d.l.

Appendix 2. Continued

Sample 512169. Central Nuuluk laminated greenschist.

sample code	169-p8	169-p9	169-p10	169-p11	169-p12	169-p16	169-p17	169-p18
mineral	ep	ep	rut	rut	rut	ep	ep	chl
SiO_2	37.99	36.88	0.14	0.04	0.11	37.85	37.59	24.88
TiO_2	0.11	0.21	96.51	96.75	96.92	0.39	0.08	0.13
Al_2O_3	26.19	23.91	0.19	0.02	0.07	24.51	25.10	22.67
Cr_2O_3	< d.l.	< d.l.	0.06	0.05	0.03	< d.l.	0.04	0.06
MgO	0.01	0.11	0.15	0.02	0.02	0.10	0.02	17.06
MnO	0.10	0.33	< d.l.	0.01	0.01	0.19	0.18	0.23
FeO	8.00	11.11	0.79	0.79	0.75	9.32	9.60	21.39
CaO	23.29	22.62	0.30	0.19	0.16	23.38	23.03	0.07
Na_2O	< d.l.	< d.l.	< d.l.	< d.l.	0.01	< d.l.	< d.l.	0.04
K_2O	0.00	0.00	0.00	0.00	0.00	0.00	0.01	0.01
F	< d.l.	< d.l.	0.10	< d.l.	< d.l.	< d.l.	< d.l.	0.01

Cations per formula unit based on: for tourmaline a Y+Z+T = 15 normalization scheme (assuming no vacancies or B in the Y, Z or T sites); to 5 cations for plagioclase; to 1 cation for rutile; to 10 cations for chlorite; and to 8 cations for epidote.

Si	3.02	2.97	0.00	0.00	0.00	3.02	3.00	2.61
Ti	0.01	0.01	0.98	0.99	0.99	0.02	0.00	0.01
Cr	2.45	2.27	0.00	0.00	0.00	2.31	2.36	2.80
Al	< d.l.	< d.l.	0.00	0.00	0.00	< d.l.	0.00	0.00
Mg	0.00	0.01	0.00	0.00	0.00	0.01	0.00	2.67
Mn	0.01	0.02	< d.l.	0.00	0.00	0.01	0.01	0.02
Fe	0.53	0.75	0.01	0.01	0.01	0.62	0.64	1.87
Ca	1.98	1.96	0.00	0.00	0.00	2.00	1.97	0.01
Na	< d.l.	< d.l.	< d.l.	< d.l.	0.00	< d.l.	< d.l.	0.01
K	0.00	0.00	0.00	0.00	0.00	0.00	0.00	0.00
F	< d.l.	< d.l.	0.00	< d.l.	< d.l.	< d.l.	< d.l.	0.00

Appendix 2. Continued

Sample 512181. Central Nuuluk laminated greenschist in thrust zone.

sample code mineral	181-1 tour	181-2 tour	181-3 tour	181-4 tour	181-5 tour	181-6 tour	181-7 tour	181-8 tour	181-9 tour	181-10 tour
SiO_2	36.64	36.64	36.78	35.98	36.82	36.93	36.26	35.59	36.32	36.53
TiO_2	0.40	0.88	0.45	0.74	0.45	0.21	0.57	0.85	0.70	0.54
Al_2O_3	31.92	31.03	32.49	30.89	31.33	31.86	31.13	30.91	31.50	32.22
Cr_2O_3	0.01	0.01	0.03	0.04	< d.l.	0.01	0.02	0.01	0.03	0.01
MgO	6.44	6.47	6.84	6.60	6.96	6.71	6.61	6.58	6.63	6.92
MnO	< d.l.	< d.l.	< d.l.	< d.l.	< d.l.	0.02	< d.l.	< d.l.	< d.l.	< d.l.
FeO	7.56	7.89	6.30	7.90	7.14	7.30	7.99	8.42	7.50	6.42
CaO	0.18	0.33	0.45	0.26	0.13	0.06	0.26	0.33	0.23	0.49
Na_2O	2.39	2.42	1.99	2.50	2.43	2.32	2.41	2.44	2.27	1.87
K_2O	0.01	0.00	0.01	0.02	0.00	0.00	0.01	0.02	0.02	0.01
F	0.08	0.11	0.10	0.14	0.13	0.09	0.09	0.10	0.11	0.19

Cations per formula unit based on: for tourmaline a Y+Z+T = 15 normalization scheme (assuming no vacancies or B in the Y, Z or T sites); to 5 cations for plagioclase/feldspar; to 1 cation for rutile; to 10 cations for chlorite; and to 8 cations for epidote.

Si	6.07	6.10	6.07	6.04	6.11	6.10	6.05	5.96	6.04	6.05
Ti	0.05	0.11	0.06	0.09	0.06	0.03	0.07	0.11	0.09	0.07
Cr	6.24	6.09	6.32	6.11	6.12	6.21	6.12	6.10	6.18	6.29
Al	0.00	0.00	0.00	0.01	< d.l.	0.00	0.00	0.00	0.00	0.00
Mg	1.59	1.61	1.68	1.65	1.72	1.65	1.64	1.64	1.64	1.71
Mn	< d.l.	< d.l.	< d.l.	< d.l.	< d.l.	0.00	< d.l.	< d.l.	< d.l.	< d.l.
Fe	1.05	1.10	0.87	1.11	0.99	1.01	1.11	1.18	1.04	0.89
Ca	0.03	0.06	0.08	0.05	0.02	0.01	0.05	0.06	0.04	0.09
Na	0.77	0.78	0.64	0.81	0.78	0.74	0.78	0.79	0.73	0.60
K	0.00	0.00	0.00	0.00	0.00	0.00	0.00	0.00	0.00	0.00
F	0.04	0.06	0.05	0.08	0.07	0.05	0.05	0.05	0.06	0.10

Appendix 2. Continued

Sample 512181. Central Nuuluk laminated greenschist in thrust zone.

sample code	181-11	181-12	181-13	181-14	181-15	181-16	181-17	181-18	181-19	181-20
mineral	tour	tour	tour	tour	tour	tour	rut	chl	chl	plag
SiO_2	36.74	36.47	36.27	35.72	36.38	36.40	0.08	26.08	26.56	53.98
TiO_2	0.62	0.57	0.62	0.59	0.65	0.48	97.00	0.02	0.12	0.01
Al_2O_3	32.46	31.99	31.96	31.52	31.63	32.79	0.09	20.28	20.50	27.82
Cr_2O_3	0.02	0.02	0.03	< d.l.	0.03	0.02	0.03	0.05	0.05	< d.l.
MgO	6.42	6.86	7.43	7.28	6.23	5.48	< d.l.	15.69	15.16	0.02
MnO	0.03	0.03	0.01	< d.l.	0.02	< d.l.	0.01	0.47	0.45	0.03
FeO	7.10	6.71	6.33	6.97	7.98	8.19	0.56	23.04	24.00	0.31
CaO	0.24	0.57	0.80	0.91	0.61	0.23	0.07	0.08	0.17	10.08
Na_2O	2.02	1.93	1.86	1.87	2.07	2.15	0.01	0.01	0.01	5.55
K_2O	0.02	0.00	0.02	0.03	0.02	0.01	0.02	0.02	0.01	0.25
F	0.03	0.09	0.16	0.13	< d.l.	0.09	< d.l.	< d.l.	< d.l.	0.04

Cations per formula unit based on: for tourmaline a Y+Z+T = 15 normalization scheme (assuming no vacancies or B in the Y, Z or T sites); to 5 cations for plagioclase/feldspar; to 1 cation for rutile; to 10 cations for chlorite; and to 8 cations for epidote.

Si	6.06	6.05	5.99	5.95	6.05	6.04	0.00	2.80	2.82	2.48
Ti	0.08	0.07	0.08	0.07	0.08	0.06	0.99	0.00	0.01	0.00
Cr	6.31	6.25	6.22	6.19	6.20	6.41	0.00	2.56	2.57	1.50
Al	0.00	0.00	0.00	< d.l.	0.00	0.00	0.00	0.00	0.00	< d.l.
Mg	1.58	1.70	1.83	1.81	1.55	1.35	< d.l.	2.51	2.40	0.00
Mn	0.00	0.00	0.00	< d.l.	0.00	< d.l.	0.00	0.04	0.04	0.00
Fe	0.98	0.93	0.87	0.97	1.11	1.14	0.01	2.07	2.13	0.01
Ca	0.04	0.10	0.14	0.16	0.11	0.04	0.00	0.01	0.02	0.50
Na	0.65	0.62	0.60	0.60	0.67	0.69	0.00	0.00	0.00	0.49
K	0.01	0.00	0.00	0.01	0.00	0.00	0.00	0.00	0.00	0.01
F	0.01	0.05	0.08	0.07	< d.l.	0.05	< d.l.	< d.l.	< d.l.	0.01

Appendix 2. Continued

Sample 512181. Central Nuuluk laminated greenschist in thrust zone.

sample code	181-21	181-22	181-23	181-24	181-25	181-26	181-27	181-28	181-29	181-l1
mineral	plag	Kspar	plag	tour	tour	tour	tour	tour	tour	tour
SiO_2	55.46	64.05	60.83	36.14	36.09	36.16	36.69	36.65	36.41	35.31
TiO_2	0.03	0.04	0.01	0.67	0.67	0.69	0.50	0.50	0.59	1.26
Al_2O_3	27.38	19.36	24.43	31.68	31.77	32.26	32.74	32.57	31.87	30.14
Cr_2O_3	0.02	< d.l.	< d.l.	0.01	0.02	0.01	0.01	0.02	0.02	0.01
MgO	< d.l.	< d.l.	< d.l.	5.87	6.09	6.34	6.02	5.99	7.38	6.20
MnO	0.01	0.03	< d.l.	< d.l.	< d.l.	< d.l.	0.03	< d.l.	0.03	0.03
FeO	0.45	0.19	0.29	8.18	8.00	7.17	7.13	7.35	6.26	9.00
CaO	9.54	0.09	4.97	0.27	0.31	0.31	0.20	0.20	0.79	0.35
Na_2O	5.90	1.54	8.74	1.95	1.98	1.97	1.77	1.77	1.99	2.37
K_2O	0.27	14.81	0.18	0.01	0.01	0.02	0.02	0.02	0.04	0.02
F	0.02	< d.l.	< d.l.	0.16	0.15	0.20	0.15	0.09	0.22	0.13

Cations per formula unit based on: for tourmaline a Y+Z+T = 15 normalization scheme (assuming no vacancies or B in the Y, Z or T sites); to 5 cations for plagioclase/feldspar; to 1 cation for rutile; to 10 cations for chlorite; and to 8 cations for epidote.

Si	2.52	2.94	2.71	6.05	6.03	6.02	6.07	6.07	6.02	5.98
Ti	0.00	0.00	0.00	0.08	0.08	0.09	0.06	0.06	0.07	0.16
Cr	1.46	1.05	1.28	6.25	6.25	6.33	6.39	6.36	6.21	6.02
Al	0.00	< d.l.	< d.l.	0.00	0.00	0.00	0.00	0.00	0.00	0.00
Mg	< d.l.	< d.l.	< d.l.	1.47	1.52	1.57	1.49	1.48	1.82	1.57
Mn	0.00	0.00	< d.l.	< d.l.	< d.l.	< d.l.	0.00	< d.l.	0.00	0.00
Fe	0.02	0.01	0.01	1.15	1.12	1.00	0.99	1.02	0.87	1.27
Ca	0.46	0.00	0.24	0.05	0.06	0.05	0.03	0.04	0.14	0.06
Na	0.52	0.14	0.75	0.63	0.64	0.64	0.57	0.57	0.64	0.78
K	0.02	0.87	0.01	0.00	0.00	0.01	0.00	0.00	0.01	0.01
F	0.00	< d.l.	< d.l.	0.09	0.08	0.11	0.08	0.05	0.12	0.07

Appendix 2. Continued

Sample 512181. Central Nuuluk laminated greenschist in thrust zone.

sample code	181-l2	181-l3	181-l4	181-l5	181-l6	181-l7	181-l8	181-l9	181-l10	181-l11
mineral	tour	tour	tour	tour	tour	tour	tour	tour	tour	tour
SiO_2	36.00	36.00	35.83	36.10	36.20	36.06	35.91	36.46	36.25	36.34
TiO_2	1.26	1.01	0.94	1.01	1.10	0.98	0.98	0.59	0.51	0.62
Al_2O_3	29.77	30.37	30.43	30.35	30.45	30.43	31.03	31.18	31.57	31.45
Cr_2O_3	< d.l.	< d.l.	0.01	0.01	0.01	0.01	0.02	0.02	0.01	0.01
MgO	6.15	6.06	6.18	6.15	6.26	6.31	6.35	5.92	5.70	5.86
MnO	0.01	< d.l.	0.02	< d.l.	< d.l.	< d.l.	0.02	< d.l.	< d.l.	< d.l.
FeO	9.01	8.91	8.72	8.56	8.69	8.54	8.00	8.39	8.76	8.41
CaO	0.36	0.30	0.30	0.32	0.35	0.30	0.23	0.17	0.21	0.26
Na_2O	2.31	2.40	2.36	2.37	2.36	2.33	2.34	2.23	2.20	2.12
K_2O	0.00	0.02	0.02	0.02	0.02	0.01	0.01	0.01	0.00	0.02
F	0.13	0.10	0.16	0.11	0.14	0.11	0.15	0.08	0.11	0.06

Cations per formula unit based on: for tourmaline a Y+Z+T = 15 normalization scheme (assuming no vacancies or B in the Y, Z or T sites); to 5 cations for plagioclase/feldspar; to 1 cation for rutile; to 10 cations for chlorite; and to 8 cations for epidote.

Si	6.08	6.06	6.04	6.09	6.07	6.06	6.03	6.11	6.06	6.08
Ti	0.16	0.13	0.12	0.13	0.14	0.12	0.12	0.07	0.06	0.08
Cr	5.93	6.03	6.05	6.03	6.01	6.03	6.14	6.16	6.22	6.20
Al	< d.l.	< d.l.	0.00	0.00	0.00	0.00	0.00	0.00	0.00	0.00
Mg	1.55	1.52	1.55	1.55	1.56	1.58	1.59	1.48	1.42	1.46
Mn	0.00	< d.l.	0.00	< d.l.	< d.l.	< d.l.	0.00	< d.l.	< d.l.	< d.l.
Fe	1.27	1.26	1.23	1.21	1.22	1.20	1.12	1.18	1.23	1.18
Ca	0.07	0.05	0.05	0.06	0.06	0.05	0.04	0.03	0.04	0.05
Na	0.76	0.78	0.77	0.77	0.77	0.76	0.76	0.72	0.71	0.69
K	0.00	0.00	0.00	0.00	0.00	0.00	0.00	0.00	0.00	0.00
F	0.07	0.05	0.09	0.06	0.08	0.06	0.08	0.04	0.06	0.03

Appendix 2. Continued

Sample 512181. Central Nuuluk laminated greenschist in thrust zone.

sample code	181-l12	181-l13	181-l14	181-l15	181-l16	181-p1	181-p2	181-p3
mineral	tour	tour	tour	tour	tour	chl	chl	Kspar
SiO_2	36.26	35.78	36.55	36.32	36.16	27.17	26.69	62.79
TiO_2	0.67	0.66	0.59	0.48	0.59	0.05	0.02	< d.l.
Al_2O_3	31.66	31.87	31.84	32.01	31.88	19.53	19.89	18.95
Cr_2O_3	0.02	< d.l.	0.01	0.01	0.03	0.03	0.06	0.01
MgO	6.06	6.06	7.04	7.20	7.16	16.51	16.71	< d.l.
MnO	< d.l.	< d.l.	0.03	< d.l.	< d.l.	0.38	0.36	0.01
FeO	8.20	7.87	6.82	6.22	6.46	23.36	22.64	0.32
CaO	0.27	0.31	0.56	0.61	0.81	0.11	0.07	0.05
Na_2O	2.06	2.08	1.95	1.92	1.92	0.01	0.01	0.31
K_2O	0.01	0.03	0.02	0.03	0.05	0.03	0.05	16.30
F	0.12	0.10	0.19	0.13	0.08	< d.l.	< d.l.	0.03

Cations per formula unit based on: for tourmaline a Y+Z+T = 15 normalization scheme (assuming no vacancies or B in the Y, Z or T sites); to 5 cations for plagioclase/feldspar; to 1 cation for rutile; to 10 cations for chlorite; and to 8 cations for epidote.

Si	6.04	6.00	6.04	6.03	6.01	2.86	2.82	2.94
Ti	0.08	0.08	0.07	0.06	0.07	0.00	0.00	< d.l.
Cr	6.22	6.30	6.20	6.26	6.24	2.43	2.48	1.04
Al	0.00	< d.l.	0.00	0.00	0.00	0.00	0.00	0.00
Mg	1.51	1.51	1.73	1.78	1.77	2.59	2.64	< d.l.
Mn	< d.l.	< d.l.	0.00	< d.l.	< d.l.	0.03	0.03	0.00
Fe	1.14	1.10	0.94	0.86	0.90	2.06	2.00	0.01
Ca	0.05	0.06	0.10	0.11	0.14	0.01	0.01	0.00
Na	0.67	0.68	0.62	0.62	0.62	0.00	0.00	0.03
K	0.00	0.01	0.01	0.01	0.01	0.00	0.01	0.97
F	0.06	0.05	0.10	0.07	0.04	< d.l.	< d.l.	0.00

Appendix 2. Continued

Sample 512181. Central Nuuluk laminated greenschist in thrust zone.

sample code	181-p4	181-p5	181-p6
mineral	rut	chl	chl
SiO_2	1.59	25.46	25.28
TiO_2	94.60	< d.l.	0.01
Al_2O_3	0.39	19.63	19.58
Cr_2O_3	0.02	0.13	< d.l.
MgO	0.03	11.51	9.04
MnO	< d.l.	0.47	0.42
FeO	0.37	29.31	33.81
CaO	0.83	0.05	0.05
Na_2O	< d.l.	< d.l.	< d.l.
K_2O	0.29	0.08	0.01
F	< d.l.	< d.l.	< d.l.

Cations per formula unit based on: for tourmaline a Y+Z+T = 15 normalization scheme (assuming no vacancies or B in the Y, Z or T sites); to 5 cations for plagioclase/feldspar; to 1 cation for rutile; to 10 cations for chlorite; and to 8 cations for epidote.

Si	0.02	2.80	2.79
Ti	0.95	< d.l.	0.00
Cr	0.01	2.54	2.55
Al	0.00	0.01	< d.l.
Mg	0.00	1.89	1.49
Mn	< d.l.	0.04	0.04
Fe	0.00	2.70	3.12
Ca	0.01	0.01	0.01
Na	< d.l.	< d.l.	< d.l.
K	0.00	0.01	0.00
F	< d.l.	< d.l.	< d.l.

Appendix 2. Continued

Electron microprobe analysis conditions:

acceleration voltage: 15kV
beam current: 20 nA
focused spot size

Element peak count times and crystal configuration

Na - 30s - TAP	Si - 20s - TAP	Mn - 50s - LIF
Mg - 30s - TAP	F - 60s - TAP	K - 50s - PETJ
Al - 20s - TAP	Fe - 30s - LIF	Ca - 40s - PETJ
Cr - 50s - LIFH	Ti - 40s - LIFH	

Standards

Na - albite	Si, Fe - olivine
Mg,Ca - diopside	F - apatite
Al, K - orthoclase	Ti - rutile
Cr - chromite	Mn - spessartine

count statistical RSD values:

SiO_2	0.7 %
TiO_2	1.5 %
Al_2O_3	0.7 %
Cr_2O_3	20 %
FeO	1.4 %
MnO	44 %
MgO	1.2 %
CaO	1.7 %
Na_2O	3.6 %
K_2O	37 %
F	1.5 %

EMP detection limits:

SiO_2	0.008 wt %
TiO_2	0.008 wt %
Al_2O_3	0.006 wt %
Cr_2O_3	0.006 wt%
FeO	0.008 wt %
MnO	0.006 wt %
MgO	0.006 wt %
CaO	0.006 wt %
Na_2O	0.005 wt %
K_2O	0.005 wt %
F	0.005 wt %

< d.l. has been substituted for values below the detection limit